

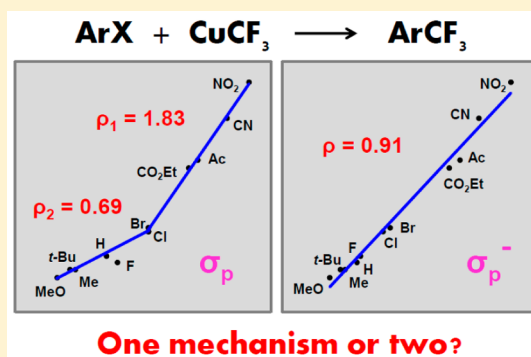
Mechanism of Trifluoromethylation of Aryl Halides with CuCF_3 and the Ortho Effect

Andrey I. Konovalov, Anton Lishchynskiy, and Vladimir V. Grushin*

Institute of Chemical Research of Catalonia (ICIQ), Av. Països Catalans 16, Tarragona, 43007 Spain

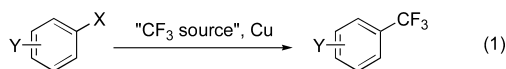
S Supporting Information

ABSTRACT: A combined experimental (radical clock, kinetic, Hammett) and computational (DFT, MM) study of the trifluoromethylation reaction of aryl halides with CuCF_3 reveals a nonradical mechanism involving Ar–X oxidative addition to the Cu(I) center as the rate determining step. The reaction is second order, first order in each reactant with $\Delta G^\ddagger \approx 24$ kcal/mol for PhI (computed $\Delta G^\ddagger = 21.9$ kcal/mol). An abrupt change in the gradient on the Hammett plot of $\log(k_R/k_H)$ versus σ_p for 11 $p\text{-RC}_6\text{H}_4\text{I}$ substrates produces two correlations ($\rho = +0.69$ and $+1.83$), which is temptingly suggestive of two different reaction pathways. Only one mechanism is operational, however, as advocated by a single linear correlation with σ_p^- ($\rho = +0.91$), analysis of the experimental ρ values, close similarity of the transition states varying in R and displaying clear signs of $-M$ interactions, and excellent reproduction of the plot by DFT. The long-known yet previously uncomprehended ortho effect has been quantified, for the first time, using the reaction of CuCF_3 with a series of $o\text{-RC}_6\text{H}_4\text{Br}$: $R(k_R/k_H) = \text{H} (1) < \text{Me} (3.5) < \text{MeO} (4) < \text{CN} (20) < \text{CHO} (250) < \text{CO}_2\text{Me} (850) < \text{NO}_2 (4300) < \text{Ac} (7300) < \text{CO}_2\text{H} (150\,000)$. With minor contributions from electronic factors, the ortho effect is largely determined by (i) the stabilizing coordination of the o -substituent to Cu in the transition state with the Cu...O distance varying directly with the barrier and (ii) the steric bulk of the o -substituent that raises the ground state free energy of the haloarene ($G^\circ_{\text{ortho}} - G^\circ_{\text{H}}$ or $G^\circ_{\text{ortho}} - G^\circ_{\text{para}}$) by inflicting molecular strain and consequently weakening the Ar–X bond.



INTRODUCTION

Since the groundbreaking discovery of the Cu-promoted perfluoroalkylation of aryl iodides by McLoughlin and Thrower¹ in the 1960s, considerable progress has been made in the area of trifluoromethylation of haloarenes with copper complexes.^{2–6} While most of the reported work targeted the development of new trifluoromethylation methodologies, surprisingly little is known about the mechanism of the copper-mediated Ar–CF₃ bond formation (eq 1). The original studies by McLoughlin and



Thrower,^{1b} Kumadaki,⁷ Yagupolskii,⁸ Kondo,⁹ Burton,¹⁰ Chen,¹¹ Tamborski,¹² Fuchikami,¹³ and others^{4,5} have provided a clear indication that the transformation involves X/CF₃ exchange on an aryl halide ArX, effected by “CuCF₃” (or “CuR_f”, where R_f = perfluoroalkyl), preformed or generated in situ from a variety of CF₃ sources. In his original seminal work, Burton¹⁰ detected three types of CuCF₃ species in solution by ¹⁹F NMR and monitored their reaction with iodoarenes. Since then, both structurally undefined CuCF₃^{4,14} and adequately characterized CF₃Cu(I) complexes [(NHC)CuCF₃],¹⁵ [(phen)CuCF₃],^{5c} [(Ph₃P)₃CuCF₃],^{5d} [(Ph₃P)(phen)CuCF₃],^{5d} and [(bathophen)CuCF₃]^{5c} (phen = 1,10-phenanthroline; bath-

ophen = bathophenanthroline) have been shown to trifluoromethylate aryl halides (mostly iodides).

While all of the reports in the area are in agreement on the order of reactivity of haloarenes ArI > ArBr > ArCl toward CF₃Cu (or R_fCu) and on the importance of amide solvents such as DMF for the reaction, there is less uniformity regarding the mechanism of the CF₃ transfer from Cu to the aromatic substrate. In the vast majority of the reports, reasonably plausible mechanisms are proposed, or no mechanistic considerations are presented whatsoever. Nonradical reaction pathways are frequently speculated to govern the Ar–CF₃ bond formation. In two instances,^{5c,i} radical clock experiments have been performed to observe the lack of formation of cyclized products and, consequently, conclude on the unlikely involvement of free radicals in the reaction. In some other cases, however, signs of single electron transfer (SET) have been observed.⁴ For example, Chen and Wu^{11b} have noted the partial suppression of the trifluoromethylation reaction of aryl iodides with FO₂SCF₂I/Cu in the presence of SET scavengers and free radical inhibitors. They have also detected the formation of a free radical addition–elimination product when performing the reaction in the presence of tetramethylethylene.

Received: July 24, 2014

Published: September 15, 2014

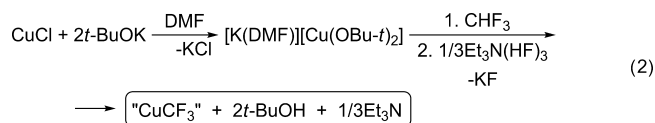
Apart from the two aforementioned radical clock experiments, the mechanism of trifluoromethylation of aryl halides has been probed by a Hammett correlation study of the decarboxylative reaction of $\text{CF}_3\text{CO}_2\text{Na}/\text{CuI}$ with a series of $p\text{-XC}_6\text{H}_4\text{I}$ ($X = \text{Me}, \text{MeO}, \text{H}, \text{F}, \text{Cl}, \text{I}, \text{CF}_3, \text{NO}_2$) in NMP at 160°C .¹⁶ From the small positive ρ value of $+0.46$ deduced, a conclusion was drawn on a nucleophilic nature of the reactive species, with $[\text{CF}_3\text{CuI}]^-$ rather than $[\text{CF}_3\text{CuI}]^\bullet$ being proposed as an intermediate. An almost identical study was most recently performed⁵¹ for the same reaction employing $\text{CF}_3\text{CO}_2\text{K}/\text{CuI}$ at 200°C for $p\text{-IC}_6\text{H}_4\text{X}$ ($X = \text{MeO}, t\text{-Bu}, \text{H}, \text{CO}_2\text{Et}$) and $m\text{-IC}_6\text{H}_4\text{CO}_2\text{Et}$. Essentially the same ρ value of $+0.52$ was obtained.

As follows from the above, there have been no reports of detailed mechanistic studies of Cu-mediated trifluoromethylation (or fluoroalkylation) of aryl halides. Considering the importance of such transformations for numerous industrial applications^{2,3} and a broad variety of possible reaction pathways for Cu-promoted aromatic coupling reactions,^{17–19} elucidation of the mechanism of the trifluoromethylation of aryl halides with CuCF_3 would benefit further developments in the area. Herein we report a combined experimental and computational study of the trifluoromethylation of haloarenes with CuCF_3 that establishes its mechanism and uncovers a number of previously unrevealed salient features of this transformation. Our work also sheds light on the nature of the so-called “ortho effect”, a long-known and widely used, yet poorly understood, accelerating effect of ortho substituents on rates of Cu-mediated coupling reactions of aryl halides. The results presented below are believed to contribute to the overall understanding of not only fluoroalkylation reactions but also aromatic substitution with copper compounds in general.

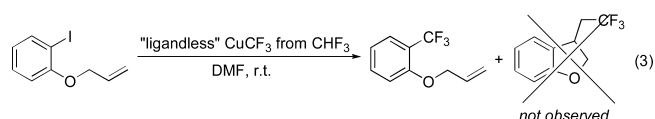
EXPERIMENTAL STUDIES

CuCF_3 Reagent. We have recently discovered^{20,21} the first reaction of direct cupration of fluoroform, established its mechanism,²² and demonstrated applications of the thus produced “ligandless” CuCF_3 for trifluoromethylation reactions of a variety of substrates.^{20–27} For the current mechanistic study, we chose the fluoroform-derived CuCF_3 reagent because of its ability to smoothly trifluoromethylate a broad variety of aryl halides in high yield and with excellent chemoselectivity under mild conditions ($20\text{--}80^\circ\text{C}$).²⁵ The CuCF_3 reagent was prepared by our previously developed procedure^{20a} in $>90\%$ yield from the reaction of CHF_3 with $[\text{K}(\text{DMF})][(\text{t-BuO})_2\text{Cu}]$ (from CuCl and 2 equiv of $t\text{-BuOK}$ in DMF), and subsequently stabilized with $\text{Et}_3\text{N}\cdot 3\text{HF}$ (eq 2). Strong evidence has been obtained^{22,27} for the original product of the cupration reaction being a mixed cuprate $[\text{K}(\text{DMF})_n][(\text{t-BuO})\text{Cu}(\text{CF}_3)]$ that undergoes acidolysis of the Cu–O bond upon the stabilization with $\text{Et}_3\text{N}\cdot 3\text{HF}$. As can be seen from the stoichiometry of the overall process (eq 2), the reagent solution thus produced contains ca. 1 equiv of “ CuCF_3 ”, 2 equiv of $t\text{-BuOH}$, and $1/3$ equiv of Et_3N . The latter two and the DMF solvent stabilize the CuCF_3 moiety by coordination through the N and O donor atoms. These interactions are rather weak, and consequently, the Et_3N , DMF, and $t\text{-BuOH}$ molecules are easily displaced from the Cu center. This is why we refer to the fluoroform-derived CuCF_3 as “ligandless”. By no means do we imply that the Cu atom in these species is monocoordinate, being devoid of any ligands but CF_3 (see below).

Radical Clock Experiment. We have previously concluded²⁵ that radical processes are unlikely involved in the trifluoromethylation of aryl halides with fluoroform-derived

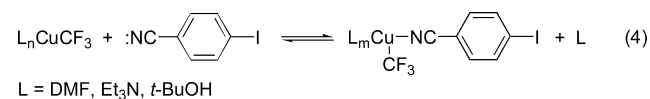


CuCF_3 . In particular, the lack of side-formation of arenes and biaryls in these reactions suggests that aryl radicals are not generated in the transformation. Furthermore, the formation of only small quantities of bis-trifluoromethylated products in the reaction of p - and o - $\text{BrC}_6\text{H}_4\text{I}$ with CuCF_3 is inconsistent with the $\text{S}_{\text{RN}}1$ mechanism.²⁸ In the current work, we found that the treatment of 2-allyloxyphenyl iodide, a radical clock substrate ($k_c = \text{ca. } 10^{10} \text{ s}^{-1}$),^{29,30} with CuCF_3 gave rise exclusively to 2-allyloxybenzotrifluoride (eq 3). No formation of the cyclized



product was observed (^{19}F NMR, GC-MS). This result provides further strong support to the previously drawn conclusion²⁵ of a nonradical mechanism of the trifluoromethylation of haloarenes with the CuCF_3 . It is worth noting that 2-allyloxyphenyl iodide has been widely used to identify radical^{26,31,32} and nonradical^{32,33} pathways for a variety of Cu-mediated reactions of aryl halides, including the trifluoromethylation with $[(\text{phen})\text{CuCF}_3]$.^{5c}

Determination of Reaction Order. The method of initial rates as measured by ^{19}F NMR was used to determine the order of the reaction of CuCF_3 with a broad variety of substrates $p\text{-RC}_6\text{H}_4\text{I}$ ($R = \text{H}, \text{Me}, \text{OMe}, \text{Cl}, \text{CO}_2\text{Et}, \text{Ac}, \text{CN}, \text{NO}_2$), $m\text{-RC}_6\text{H}_4\text{I}$ ($R = \text{Me}, \text{OMe}, \text{Cl}, \text{CHO}, \text{CO}_2\text{Et}, \text{CN}, \text{NO}_2$), $o\text{-NCC}_6\text{H}_4\text{I}$, and $o\text{-RC}_6\text{H}_4\text{Br}$ ($R = \text{CO}_2\text{Me}, \text{CHO}, \text{Ac}, \text{CN}, \text{NO}_2$). In the range of concentrations of CuCF_3 and ArX 0.095–0.380 M, all but two reactions exhibited clean second order kinetics, first order with respect to each reactant. Deviations from the second order were observed for $p\text{-IC}_6\text{H}_4\text{CN}$ and $p\text{-IC}_6\text{H}_4\text{NO}_2$. With these two aryl iodides, the reaction was ca. 0.5 order with respect to both the substrate and CuCF_3 . We reasoned that the deviation might deal with the reversible coordination of the CN and NO_2 groups on the substrate to the Cu center, as shown in eq 4 for $R = \text{CN}$.³⁴ To



probe this hypothesis, we repeated the reaction order determination for $p\text{-IC}_6\text{H}_4\text{CN}$ and $p\text{-IC}_6\text{H}_4\text{NO}_2$ in the presence of MeCN in excess. Being a better ligand for Cu(I) than $p\text{-IC}_6\text{H}_4\text{R}$ ($R = \text{CN}$ or NO_2), DMF, $t\text{-BuOH}$, and Et_3N , acetonitrile was expected to free up the substrate from its Cu complex and drive all ligand exchange equilibria in the system to $[(\text{MeCN})_n\text{-Cu}(\text{CF}_3)]$. Indeed, in the presence of MeCN (50 equiv per Cu), both reactions displayed second order kinetics, first order in Cu and first order in $p\text{-IC}_6\text{H}_4\text{R}$ ($R = \text{CN}$ or NO_2). The addition of MeCN not only restored the second order of the reaction, but also slowed the trifluoromethylation by a factor of 4.5. The observed slower rates are consistent with the previously reported^{5d,25} inhibition of trifluoromethylation reactions of aryl halides with CuCF_3 complexes in the presence of deliberately added ligands with a high affinity for Cu(I). Second order kinetic behavior was invariably observed for the reactions of all of the $o\text{-RC}_6\text{H}_4\text{Br}$ and $m\text{-RC}_6\text{H}_4\text{I}$ substrates with CuCF_3 in DMF in the absence of MeCN. The lack of deviation from the first order in

CuCF₃ and in *o*-RC₆H₄X (X = Br, I) or *m*-RC₆H₄I for R = CN and NO₂ is attributed to an expected³⁵ weaker binding of the Cu to these groups, as compared with those in the para derivatives *p*-IC₆H₄NO₂ and *p*-IC₆H₄CN (eq 4).

Hammett Studies. The Para Series. Relative rate constants were determined for the reactions of CuCF₃ with 11 iodoarenes *p*-RC₆H₄I (R = H, Me, *t*-Bu, MeO, F, Cl, Br, CO₂Et, Ac, CN, and NO₂) at 298 K. The reactions of CuCF₃ in DMF with two or more competing aryl iodides were run under pseudo-first-order conditions with [*p*-XC₆H₄I]/[CuCF₃] = 10 for each substrate and monitored by ¹⁹F NMR. Two sets of experiments were performed. In one, the reactions for all 11 substrates were run in the presence of MeCN (50 equiv per Cu) in order to avoid the above-described deviation from second order kinetics for R = CN and NO₂. The second set of measurements was performed in the absence of MeCN. Within each data set, different runs performed at various concentrations and conversions showed excellent reproducibility and no variation in *k_R/k_H* within the estimated experimental error of ca. 10%. Notably, the same decrease in the reaction rates by a factor of 4.5 in the presence of 50 equiv of MeCN (see above) was observed for all substrates in the series. Consequently, the *k_R/k_H* values obtained in the presence and in the absence of MeCN were indistinguishable within the experimental error.

Unexpectedly, plotting the log(*k_R/k_H*) values against the Hammett σ_p constants³⁶ resulted in no satisfactory linear correlation. Excellent correlations were obtained, however, for two separate sets within the series (Figure 1, top), one with R = H, Me, *t*-Bu, MeO, Cl, and Br ($\rho = +0.69 \pm 0.01$; $R^2 = 0.99$) and the other with R = F, Cl, Br, CO₂Et, Ac, CN, and NO₂ ($\rho = +1.83 \pm 0.01$; $R^2 = 1.00$). While we are unaware of similar observations in the chemistry of Cu-catalyzed reactions of aryl halides,^{5j,37–44} a strikingly similar Hammett pattern with an abrupt line breakage at about the same point, $\sigma_p = +0.23$ (Cl), has been reported by Foà and Cassar⁴⁵ for Ar–Cl oxidative addition to [(Ph₃P)₃Ni]. That dual correlation pattern was convincingly interpreted in terms of two different mechanisms governing the transformation. On the other hand, we found that our log(*k_R/k_H*) values correlate excellently ($\rho = +0.91 \pm 0.01$; $R^2 = 0.99$) with σ_p^- (Figure 1, bottom), a parameter that is conventionally used for reactions where considerable negative resonance interaction takes place between the substituent and the reaction center.³⁶

Hammett Studies. The Meta Series. An excellent linear correlation of the log(*k_R/k_H*) values with the Hammett σ_m constants³⁶ was obtained for the reactions of CuCF₃ with eight iodoarenes *m*-RC₆H₄I (R = H, Me, MeO, CO₂Et, CHO, Cl, CN, and NO₂) at 298 K. Although all of these reactions obeyed second order kinetics in the absence of MeCN (see above), the *k_R/k_H* determination was repeated in the presence of 50 equiv of MeCN for comparison with the para series. As with the *p*-RC₆H₄I substrates, the addition of MeCN slowed down all of the reactions by the same factor of 4.5. As a result, the Hammett plots for the reactions in the presence of MeCN ($\rho = +0.95 \pm 0.03$; $R^2 = 0.99$) and in its absence ($\rho = +0.97 \pm 0.03$; $R^2 = 0.99$) were virtually indistinguishable (Figure 2).

Ortho Effect. Originally discovered by Ullmann himself 110 years ago,⁴⁶ the remarkable promoting effect of certain ortho substituents such as COOH and NO₂ on Cu-catalyzed/mediated coupling reactions of aryl halides has long been recognized.^{47,48} Clark and co-workers⁴⁹ have observed the ortho effect of a nitro group on the trifluoromethylation of aryl chlorides with CuCF₃ generated from Cu and CF₂Br₂ in DMAC. A much weaker reaction rate enhancement was detected for carbonyl ortho

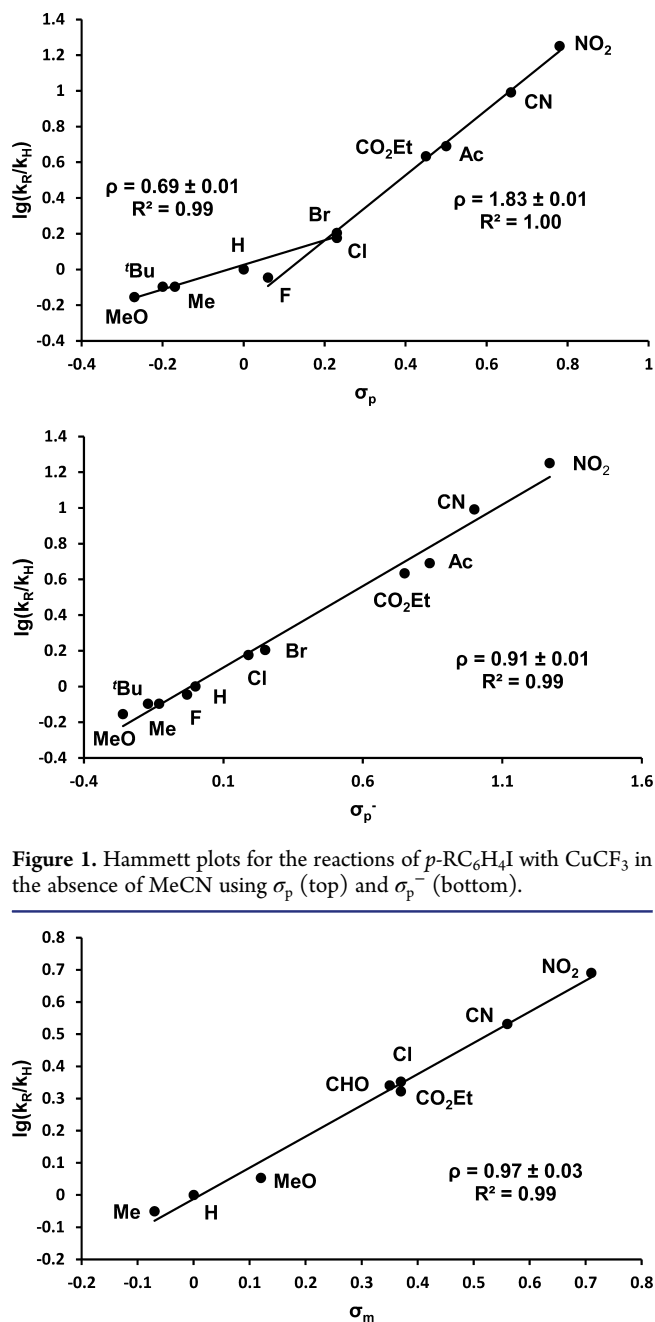


Figure 1. Hammett plots for the reactions of *p*-RC₆H₄I with CuCF₃ in the absence of MeCN using σ_p (top) and σ_p^- (bottom).

Figure 2. Hammett plot for the reactions of *m*-RC₆H₄I with CuCF₃ (in the absence of MeCN).

substituents CHO, Ac, and CO₂Me, whereas the cyano and amino groups in the ortho position did not alter the reactivity of the C–Cl bond. Following the previously reported explanations,^{47,48} Clark rationalized the lack of ortho effect of the cyano group in terms of the unattainability of “the correct transition state geometry” as shown in Figure 3.⁴⁹

In Clark’s studies, the ortho effect could not be explored for aryl iodides and bromides as those produced biaryls rather than trifluoromethylated products under the conditions employed.⁴⁹ We have recently observed²⁵ the ortho effect in the trifluoromethylation reactions of both aryl iodides and bromides with fluoroform-derived CuCF₃. In the current work, this effect has been studied and quantified for a series of bromoarenes. Relative rate constants were determined by ¹⁹F NMR for

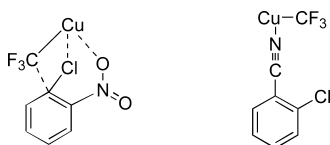


Figure 3. Proposed⁴⁹ “correct” (*ortho*-NO₂) and “incorrect” (*ortho*-CN) geometries of the transition states in the Cu-promoted trifluoromethylation of *ortho*-substituted chloroarenes.

trifluoromethylation of a series of *ortho*-substituted bromoarenes in competition experiments where 1 equiv of CuCF₃ was allowed to react with a mixture of various *o*-RC₆H₄Br (10 equiv of each) under pseudo-first-order conditions. Aryl bromides rather than iodides were chosen for this study in order to have a broader range of substrates in the series. Preliminary runs had indicated that some *o*-RC₆H₄I (e.g., R = CO₂H, Ac, CO₂R, NO₂) appeared too reactive toward the CuCF₃ (relative to PhI) for accurate k_R/k_H determination. Monitoring the reactions by ¹⁹F NMR and integration of the peaks from the *o*-RC₆H₄CF₃ products gave the following order of reactivity with relative rate constants shown in parentheses: H (1) < Me (3.5) < MeO (4) < CN (20) < CHO (250) < CO₂Me (850) < NO₂ (4300) < Ac (7300) < CO₂H (150 000).

This order of reactivity displays a number of peculiar features:

(1) There is no correlation of the relative rate constants with the electronic effects³⁶ of R. The carboxyl group displaying by far the strongest *ortho* effect is a weaker electron acceptor than Ac, CN, and NO₂. The cyano group is a more powerful electron-acceptor than any of the carbonyl substituents that nonetheless make the substrate more reactive. While the nitro group is more electron-withdrawing than acetyl, *o*-bromoacetophenone reacts with CuCF₃ faster than *o*-bromonitrobenzene.

(2) In contrast with Clark's observations,⁴⁹ the acetyl group is a noticeably stronger *ortho* activator than the nitro group.

(3) Astonishingly, even a methyl group *ortho* to the C–Br bond promotes the reaction, as can be seen from 2-bromotoluene being 3.5 times more reactive toward the CuCF₃ than bromobenzene. This is particularly unexpected as the CH₃ substituent is neither an electron-acceptor to activate the carbon–halogen bond on the ring, nor a lone electron pair donor to bind to the Cu atom, thereby bringing it in closer proximity to the reaction site (Figure 3). A similar weak yet recognizable effect of the methyl group has also been observed in the 3-bromopyridine series.²⁵ Furthermore, bromomesitylene bearing two methyl groups *ortho* to the C–Br bond appeared 1.3 and 4.5 times more reactive than 2-bromotoluene and bromobenzene, respectively.

COMPUTATIONAL STUDIES

The “one or two mechanisms” dilemma (Figure 1) could not be solved by experimental methods, and the *ortho* effect could not be rationalized only in terms of relative electron deficiency of the aromatic substrates, nor solely in terms of chelation as previously proposed.^{48,49} We therefore undertook a series of computational studies to gain a deeper insight into the mechanism of the reactions of CuCF₃ with aryl halides and the nature of the *ortho* effect. Density functional theory (DFT) calculations based on a mPW2PLYPD(BS2)//B3LYP-D(BS1) protocol have been used throughout the study. In the following sections, all energies correspond to computed Gibbs free energies in DMF, unless noted otherwise.

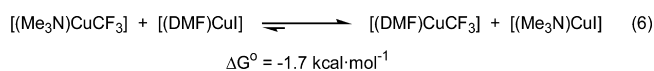
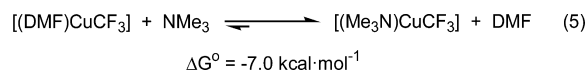
Model Selection. As discussed above, after the cupration of fluoroform and stabilization of the trifluoromethyl Cu(I) complex produced with Et₃N·3HF, the resultant reagent solution in DMF comprises “CuCF₃”, *t*-BuOH, and Et₃N in a 1:2:0.33 molar ratio (eq 2). Given that and the consensus^{33b,d,50} that the reactive species in Ullmann-type reactions are complexes of the type [(L)Cu(nucleophile)], we considered [LCuCF₃] (L = DMF, *t*-BuOH, Et₃N) as the CF₃-transferring molecules. The computed bond dissociation free energies (BDFE) showed that Et₃N (modeled as Me₃N) binds to CuCF₃ 7.0 kcal/mol more strongly and *t*-BuOH 2.1 kcal/mol less strongly than DMF (Table 1).⁵¹

Table 1. L–CuCF₃ Bond Dissociation Free Energies (BDFEs)

ligand L	L:CuCF ₃ molar ratio	BDFE, kcal mol ⁻¹
DMF	ca. 28 ^a	20.5
<i>t</i> -BuOH	2	18.4
NEt ₃ ^b	0.33	27.5

^aCalculated from the actual concentration of CuCF₃ solutions used in the experimental studies. ^bModeled as NMe₃.

In spite of the large DMF to Et₃N molar ratio of ca. 85:1 under the experimental conditions, the computed data indicate that the equilibrium between [(DMF)CuCF₃] and [(Me₃N)CuCF₃] (eq 5) in the CuCF₃ reagent solution is shifted almost entirely to the amino complex. Nevertheless, the species selected for the computational studies was [(DMF)CuCF₃] because the actual reagent solution contains only ca. 0.33 equiv of Et₃N per each equiv of CuCF₃, whereas the DMF solvent is abundant (see above and eq 2). Furthermore, as the reaction with an aryl iodide occurs, CuI is produced that binds⁵² to the tertiary amine more strongly than CuCF₃ (eq 6). Finally, as will be shown below, the selected model species [(DMF)CuCF₃] is more reactive toward ArX than [(Me₃N)CuCF₃]. The complex bearing two DMF ligands on Cu, [(DMF)₂CuCF₃], was computed to lie 6.0 kcal/mol higher in energy than [(DMF)CuCF₃] and therefore was disregarded in the DFT study. Consequently, all energies in the DFT study are quoted relative to the combined Gibbs free energies of [(DMF)CuCF₃] and the corresponding aryl halide set to zero.



Trifluoromethylation of PhI. Associative and Dissociative Oxidative Addition–Reductive Elimination Pathways. Initially, we studied the reaction of [(DMF)CuCF₃] with the simplest iodoarene, PhI, as a model substrate. The reaction of fluoroform-derived CuCF₃ with PhI has been experimentally shown²⁵ to cleanly produce PhCF₃ in 95% yield at 99% conversion after 18 h at 50 °C. First we probed a mechanism involving Ph–I oxidative addition (OA) to produce a Cu(III) species, followed by Ph–CF₃ reductive elimination (RE). Two alternative computed pathways for this process are shown in Figure 4. One of them (dissociative, shown in blue) involves DMF loss from Cu as the first step, whereas the other one (associative, shown in red) does not.

In the dissociative OA-RE pathway (DOARE), the [(PhI)CuCF₃] adduct in its most stable form [D]I_{1a} (8.3 kcal/mol)

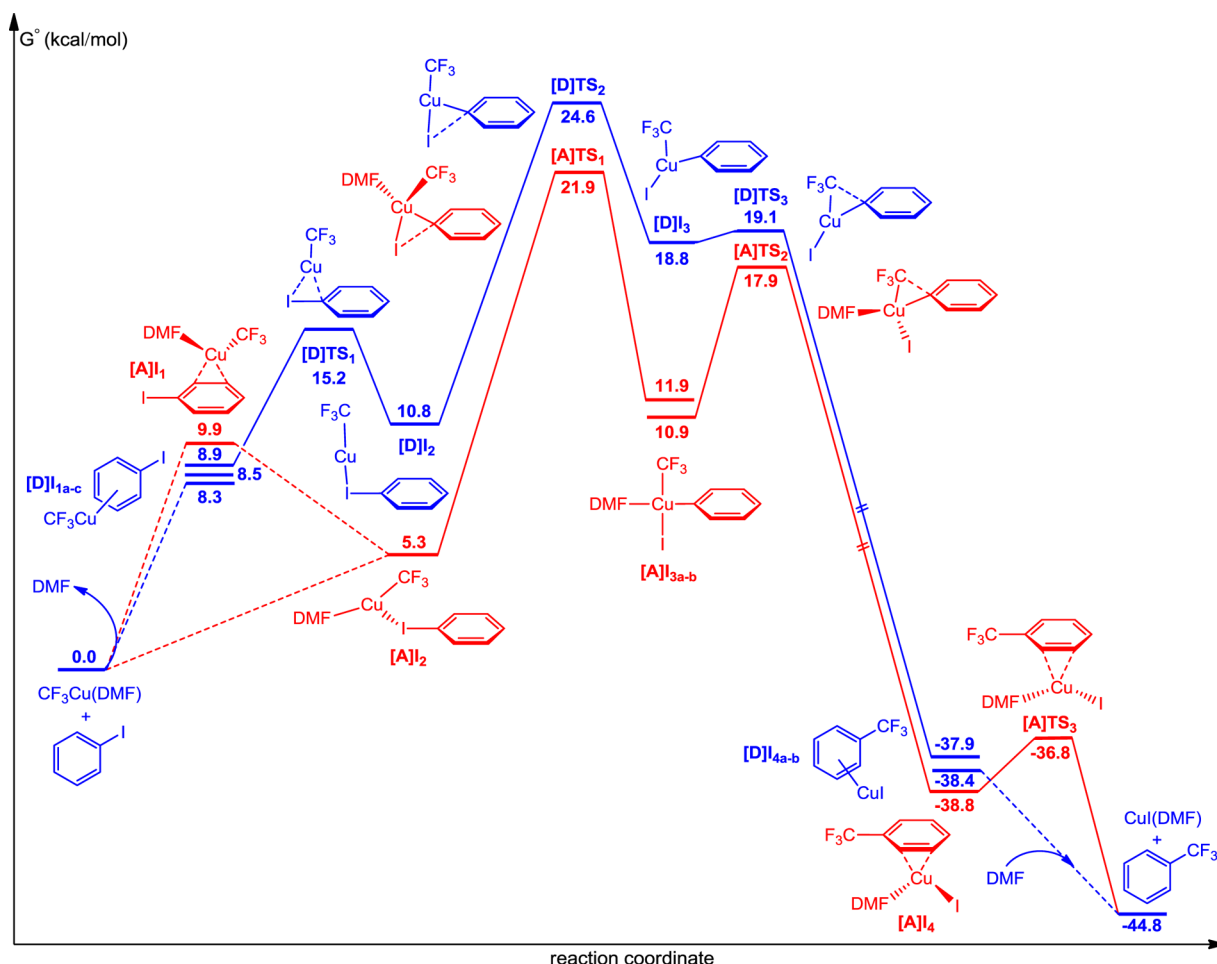


Figure 4. Alternative computed reaction profiles for the reaction of $[(\text{DMF})\text{CuCF}_3]$ with PhI via OA-RE involving (blue, "DOARE") and not involving (red, "AOARE") DMF dissociation.

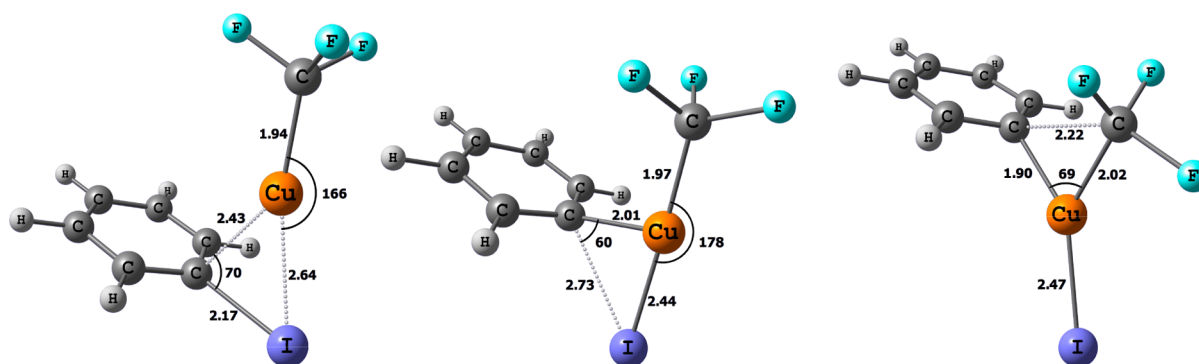


Figure 5. Computed DOARE transition states for (left) CuCF_3 transfer from the π -system to iodine ($[\text{D}]\text{TS}_1$; 15.2 kcal/mol), (center) Ph-I OA to CuCF_3 ($[\text{D}]\text{TS}_2$; 24.6 kcal/mol), and (right) Ph- CF_3 RE from Cu ($[\text{D}]\text{TS}_3$; 19.1 kcal/mol).

exhibits an η^2 -binding mode through one $\text{C}_{\text{meta}}-\text{C}_{\text{para}}$ bond. Alternative η^2 -arene species $[\text{D}]\text{I}_{1\text{b}}$ and $[\text{D}]\text{I}_{1\text{c}}$ bound through either a $\text{C}_{\text{ortho}}-\text{C}_{\text{meta}}$ or a $\text{C}_{\text{ipso}}-\text{C}_{\text{ortho}}$ bond are only slightly higher in energy, by 0.2 and 0.6 kcal/mol, respectively. The CuCF_3 coordination to the $\text{C}_{\text{para}}-\text{C}_{\text{meta}}$ or $\text{C}_{\text{meta}}-\text{C}_{\text{ortho}}$ bonds leads to a shortening of the C-I bond by 0.1 Å ($\text{C}-\text{I} = 2.14$ Å in free PhI), likely due to electron donation from the π system of the benzene ring to the Lewis-acidic copper atom. In contrast, in the $\text{C}_{\text{ortho}}-\text{C}_{\text{ipso}}$ adduct $[\text{D}]\text{I}_{1\text{c}}$, the C-I bond is elongated by 0.1 Å and the iodine atom deviates from the plane of the benzene ring by 10° . This distortion is indicative of predominant binding of

Cu to the ipso C atom, the reactive site of the substrate, i.e., of Ph-I preactivation. CuCF_3 transfer from the π -system in $[\text{D}]\text{I}_{1\text{c}}$ to the iodine through a low-energy transition state $[\text{D}]\text{TS}_1$ (15.2 kcal/mol; Figure 5, left) leads to further elongation of the C-I bond and the formation of a σ -complex with a nearly linear $\{\text{F}_3\text{C}-\text{Cu}-\text{I}\}$ moiety orthogonal to the benzene ring (93°). Characterization of the subsequent C-I activation transition state showed that this I-bound intermediate $[\text{D}]\text{I}_2$ is the immediate precursor in this process. The Ph-I OA proceeds via a relatively late transition state $[\text{D}]\text{TS}_2$ (24.6 kcal/mol; Figure 5, center) with significant C \cdots I elongation (2.73 Å), a short $\text{Cu}\cdots\text{Ph}$

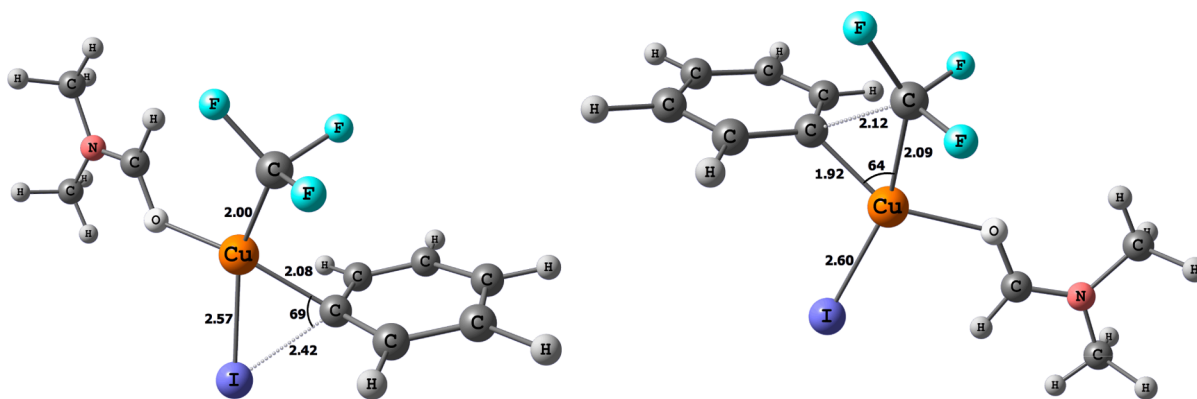


Figure 6. Computed AOARE transition states (left) for Ph–I OA to [(DMF)CuCF₃] ([A]TS₁; 21.9 kcal/mol) and (right) Ph–CF₃ RE from Cu ([A]TS₂; 17.9 kcal/mol).

contact (2.01 Å), and a short Cu–I bond distance (2.44 Å) that is only 0.1 Å longer than in copper iodide. C–I bond cleavage within the near-linear {F₃C–Cu–I} moiety (178°) with the Ph group effectively bridging the Cu–I bond leads to a Cu(III) Y-shaped intermediate, [D]I₃ (18.8 kcal/mol) with an acute Ph–Cu–CF₃ angle of 77° and a Ph⋯CF₃ contact of 2.4 Å. This geometry facilitates the Ph–CF₃ RE step via [D]TS₃ (19.1 kcal/mol; Figure 5, right) with a minimal barrier of 0.3 kcal/mol and results in a dramatic lowering of energy and the formation of a η²-intermediate ([D]I_{4a}, –37.9 kcal/mol) with CuI π-bound to C_{ortho}–C_{meta} of the PhCF₃ molecule produced. After a rearrangement to the C_{meta}–C_{para} isomer [D]I_{4b} (–38.4 kcal/mol), DMF coordination to the CuI liberates the PhCF₃ molecule.

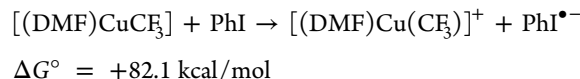
In the associative OA-RE pathway (AOARE; shown in red in Figure 4), PhI can π-coordinate to [(DMF)CuCF₃] to produce a η²-C_{meta}–C_{ortho} complex [A]I₁ at 9.9 kcal/mol or form a more stable iodine-bound σ-complex [A]I₂ (5.3 kcal/mol). The latter displays a nearly linear {(DMF)CuCF₃} fragment (179°), a long Cu⋯I distance (3.61 Å), and a C–I bond that is almost indistinguishable in length (2.14 Å) from that in free PhI. This weak adduct is connected to an OA transition state [A]TS₁ (21.9 kcal/mol). The C⋯I (2.42 Å) and Cu⋯I (2.57 Å) contacts computed for [A]TS₁ (Figure 6, left) are shorter and longer, respectively, than in [D]TS₂ (C⋯I = 2.73 Å; Cu⋯I = 2.44 Å), indicating that Ph–I activation via AOARE is governed by an earlier transition state than in DOARE. This leads to a pathway that is energetically lower by 2.7 kcal/mol for the trifluoromethylation with [(DMF)CuCF₃] than with [CuCF₃]. Descent from [A]TS₁ yields an intermediate [A]I_{3a} with square-planar Cu(III) (Ph–Cu–I = 90°) at 11.9 kcal/mol that rearranges to a slightly more stable conformer [A]I_{3b} (10.9 kcal/mol) via rotation around the DMF–Cu bond. Involvement of high spin Cu(III) species can be ruled out as optimization of the originally produced d⁸ Cu(III) intermediate in a triplet state produced an energetically prohibited distorted tetrahedral structure at +46.0 kcal/mol.

RE from the Cu(III) intermediate [A]I_{3b} that is lower in energy than [D]I₃ is favored by the formation of a strong Ph–CF₃ bond and occurs with a small barrier of 7.0 kcal/mol via [A]TS₂ (17.9 kcal/mol), a transition state that is also lower in energy than its DOARE congener [D]TS₃. The resultant intermediate [A]I₄ comprised a {I–Cu–DMF} moiety η²-bound to a C_{ortho}–C_{meta} bond of PhCF₃ loses the latter via [A]TS₃. This dissociation process characterized by a very low barrier of only 2 kcal/mol completes the transformation. The

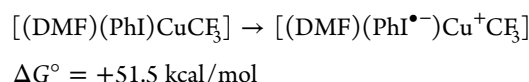
calculated overall free energy effect of –44.8 kcal/mol shows that the trifluoromethylation process is highly exergonic.

Alternative Mechanisms. A recent computational study^{19a} of Ph–I activation with [(L-L)Cu(ZMe)] (L-L = diketone or phen; Z = O, NH) showed that single electron transfer (SET) and halogen atom transfer (HAT) processes can be competitive with concerted oxidative addition. Therefore, these alternatives to the OA-RE mechanism as well as σ-bond metathesis (SBM) and S_NAr were also considered, focusing on the Ph–I activation step. For SBM, the computed barrier was 64.5 kcal/mol. The other alternatives were assessed by computing the standard free Gibbs energy change for the following Ph–I activation steps:

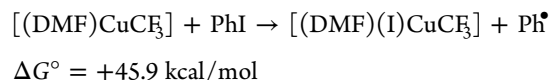
SET(outer sphere):



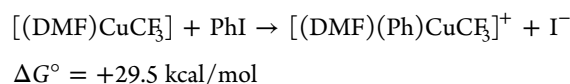
SET(inner sphere):



HAT:



S_NAr:



The high computed ΔG° values suggest that these mechanisms are not relevant in the present system.

Para-Substituted Aryl Iodides. The above-described OA-RE model (Figure 4) was then applied to a range of *p*-RC₆H₄I substrates, for which relative rates were determined experimentally (see above). Both the DOARE and AOARE pathways were studied for the entire series. The key transition states [D]TS₂ and [A]TS₁ computed for the substituted aryl iodides displayed geometries that were similar to those found for iodobenzene. The energy values presented below correspond to the most stable conformers in all cases.

For DOARE, the computed barriers (in kcal/mol in parentheses) produced the following order of reactivity: NO₂

(25.8) < CO₂Et (25.6) < CN (25.5) < Ac (25.4) < Cl (25.2) < MeO (25.1) < Br (25.0) < F (24.9) < Me (24.6) ≈ H (24.6) < *t*-Bu (24.3). This sequence suggests that electron-withdrawing substituents in the para position would produce slower reaction, which is the opposite of the experimentally observed trend. Attempted correlation of σ_p^- with the $\log(k_R/k_H)$ numbers derived from the computed data produced an unrealistic negative⁵³ ρ value of -0.56 (Figure 7).

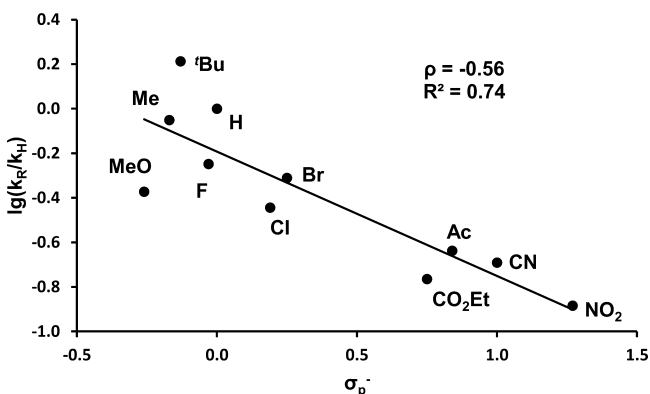


Figure 7. Hammett plot of DFT computation-derived $\log(k_R/k_H)$ vs σ_p^- for the reactions of *p*-RC₆H₄I with CuCF₃ via DOARE.

In sharp contrast, the order of reactivity predicted by the theory for the AOARE pathway (computed barriers in kcal/mol in parentheses), Me (22.8) < MeO (22.6) < F (22.4) < *t*-Bu (22.0) ≈ Cl (22.0) ≈ Br (22.0) < H (21.9) < Ac (22.5) < CO₂Et (21.4) < CN (21.1) < NO₂ (20.3), accords with the experimental data. In spite of a few minor deviations, a much better correlation of the DFT-derived $\log(k_R/k_H)$ values with σ_p^- is observed, producing $\rho = +0.92$ (Figure 8) that is in excellent agreement with the experimental value of $+0.91$ (Figure 1, bottom).⁵⁴

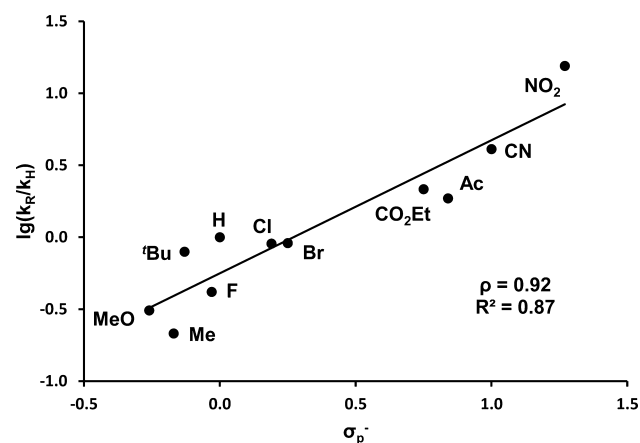


Figure 8. Hammett plot of DFT computation-derived $\log(k_R/k_H)$ vs σ_p^- for the reactions of *p*-RC₆H₄I with CuCF₃ via AOARE.

The computational results described above indicate that the DOARE pathway is not only energetically more demanding than AOARE, but also not consistent with the experimental Hammett data, whereas AOARE is. This applies to correlations of the DOARE and AOARE $\log(k_R/k_H)$ values not only with the resonance constant σ_p^- but also with the Hammett σ_p parameter (see the Supporting Information). Therefore, only the AOARE

mechanism was considered for the computational Hammett modeling of the meta series.

Meta-Substituted Aryl Iodides. The experimentally established susceptibility of the trifluoromethylation of *m*-RC₆H₄I to R (σ_m) is particularly low, as illustrated by the most rapid reaction (R = NO₂) being only 5.5 times faster than the slowest one (R = Me). The Arrhenius equation translates this rate constant ratio into 1.0 kcal/mol for the entire range of ΔG^\ddagger in the reactions of the meta series. Given this very small value, it was hard to expect DFT calculations to reproduce the experimentally obtained Hammett plot (Figure 2). To our delight, however, the computed barriers (kcal/mol in parentheses) for the AOARE pathway, Me (22.7) < CHO (22.2) ≈ CN (22.2) < Cl (22.1) < H (21.9) ≈ MeO (21.9) ≈ CO₂Et (21.9) < NO₂ (21.8), appeared to be in good agreement with the experimental order of reactivity. While the difference of 0.1 kcal/mol or less for the neighboring members of the series is computationally insignificant, the DFT method identified correctly the most and the least reactive substrates and modeled well the small 0.9 kcal/mol difference in the Gibbs free energies of activation for the two.

Additional Calculations Related to the AOARE Mechanism. We have also computed barriers to OA of PhBr and PhCl to [(DMF)CuCF₃]. The values obtained, 25.1 kcal/mol (PhBr) and 28.8 kcal/mol (PhCl), accord with the experimentally observed order of reactivity PhI > PhBr > PhCl. These data confirm that the rate limiting step of the trifluoromethylation of aryl halides with CuCF₃ is activation of the carbon–halogen bond.

The replacement of DMF in [(DMF)CuCF₃] with NMe₃ in the calculations with PhI as the substrate raises the activation barrier by 2.4 kcal/mol. Using the Arrhenius equation, this figure translates into [(Me₃N)CuCF₃] being ca. 60 times less reactive toward PhI than [(DMF)CuCF₃]. These data are consistent with the experimentally observed²⁵ inhibiting effect of triethylamine on the trifluoromethylation of aryl halides with fluoroform-derived CuCF₃.

It has been well-established^{4,10,14} that under certain conditions CuCF₃ can exist in equilibrium with [Cu(CF₃)₂]⁻ that is less reactive toward haloarenes.^{15b} Computing a barrier to the AOARE pathway for PhI involving [Cu(CF₃)₂]⁻ as a trifluoromethylating agent produced a high value of 28.1 kcal/mol, in full accord with the experimental data.^{15b} One can imagine that [Cu(CF₃)₂]⁻ might react with CuI coproduced in the reaction to give rise to [(CF₃)CuI]⁻ that might also react with the aromatic iodide. In fact, [(CF₃)CuI]⁻ has been proposed¹⁶ as the reactive species in the decarboxylative trifluoromethylation of iodoarenes. However, the computed AOARE barrier for Ph-I OA to [(CF₃)CuI]⁻ (25.3 kcal/mol) is 3.4 kcal/mol higher than to [(DMF)CuCF₃] (21.9 kcal/mol).

The Ortho Effect. First we computed the oxidative addition transition states for the reactions of the entire series of ortho-substituted bromoarenes used in the experimental studies with [(DMF)CuCF₃] via the AOARE pathway. As can be seen from Table 2, the DFT values for the difference in the Gibbs free energies for the transition states involving PhBr ΔG^\ddagger_H and *o*-RC₆H₄Br ΔG^\ddagger_R are in good agreement with those calculated from the experimental kinetic data. The overall trend is reproduced remarkably well by the computation with only one minor exception (R = CN) that, considering the accuracy of the DFT method, may not be viewed as significant. The consonant experimental and computational data show that the introduction of a substituent into an ortho position of PhBr enhances the

Table 2. Experimental and DFT Data for the Ortho Effect in the Reactions of *o*-RC₆H₄Br with CuCF₃

R	<i>k_R</i> / <i>k_H</i> (expt)	$\Delta G_{\text{H}}^{\ddagger} - \Delta G_{\text{R}}^{\ddagger}$ (kcal/mol)	
		expt	DFT
H	1	0.0	0.0
Me	3.5	0.7	0.6
MeO	4	0.8	1.2
CN	20	1.7	1.1
CHO	250	3.2	3.2
CO ₂ Me	850	3.9	5.4
NO ₂	4300	4.9	5.6
Ac	7300	5.2	6.1
CO ₂ H ^a	150 000	6.9	7.0

^aComputed for the ionized form.

reactivity of the bromoarene toward CuCF₃. The magnitude of the effect strongly depends on the nature of R and, as mentioned above, does not correlate with its electronic effects.

To gain insight into the origin of the ortho effect, we calculated AOARE transition states for the oxidative addition of *o*-RC₆H₄I to [(DMF)CuCF₃], the highest energy point on the reaction coordinate, and compared them with those previously computed for the corresponding para isomers. As the overall reaction barrier for a transformation is determined by the difference in energies of the reactants and the transition state, we also computed and compared *G*^o for each *o*-RC₆H₄I/*p*-RC₆H₄I pair. Results of these studies are summarized in Table 3. Similar to the

Table 3. Computed Energy Parameters (kcal/mol) for *o*- and *p*-RC₆H₄I and Their Reactions with [(DMF)CuCF₃]

R	$G_{\text{para}}^{\text{ortho}} - G_{\text{para}}^{\text{ortho}}$	$\Delta G_{\text{ortho}}^{\ddagger}$	$\Delta G_{\text{para}}^{\ddagger}$	$\Delta G_{\text{ortho}}^{\ddagger} - \Delta G_{\text{para}}^{\ddagger}$	$\Delta G_{\text{H}}^{\ddagger} - \Delta G_{\text{ortho}}^{\ddagger}$	$G_{\text{ortho}}^{\ddagger} - G_{\text{para}}^{\ddagger}$
H	0.0	21.9	21.9	0.0	0.0	0.0
F	0.5	21.9	22.4	0.5	0.0	0.0
CN	0.8	20.5	21.1	0.6	1.4	0.3
Br	2.1	20.9	21.9	1.0	1.0	1.0
Cl	1.9	20.6	21.9	1.3	1.3	0.5
MeO	0.6	20.8	22.6	1.8	1.1	-1.1
Me	1.1	20.9	22.8	1.9	1.0	-0.8
CHO	2.8	19.2	21.9	2.7	2.7	0.1
NO ₂	5.4	17.4	20.3	2.9	4.5	2.5
CO ₂ Et	4.5	17.8	21.4	3.6	4.1	0.9
Ac	5.1	15.8	21.5	5.7	6.1	-0.6
CO ₂ H ^a	2.5	15.1	22.7	7.6	6.8	-5.1

^aComputed for the ionized form.

ortho-substituted aryl bromide series (Table 2), the ortho effect is observed in all cases, i.e., $\Delta G_{\text{H}}^{\ddagger} - \Delta G_{\text{ortho}}^{\ddagger}$ is always a positive value, except for the smallest substituent, F, where it is essentially zero. The computed AOARE barriers are also always lower for the ortho-substituted substrates than for their para isomers.

As can be seen from Table 3 and in accord with the literature data,⁵⁵ all of the ortho isomers studied lie invariably higher in energy than the corresponding para isomers. The $G_{\text{ortho}}^{\text{ortho}} - G_{\text{para}}^{\text{ortho}}$ values for the series vary in a significant range 0.5–0.6 kcal/mol (F, MeO) to 5.1–5.4 kcal/mol (Ac, NO₂). This difference in the ground state energies between the ortho and para isomers is one of the two intrinsic contributors to the ortho effect. The other parameter determining the barrier is the difference in the energies of the transition states, $G_{\text{ortho}}^{\ddagger} - G_{\text{para}}^{\ddagger}$, reflecting the degree of stabilization or destabilization upon moving R from the

para to the ortho position. As can be seen from Table 3, this para–ortho “isomerization” of the AOARE transition state after full optimization can be stabilizing (R = Me, MeO, Ac, CO₂⁻), destabilizing (R = Cl, CO₂Et, CN, NO₂, Br, CHO), or energy-neutral (R = F). Importantly, however, the difference $G_{\text{ortho}}^{\text{ortho}} - G_{\text{para}}^{\text{ortho}}$ is always larger than $G_{\text{ortho}}^{\ddagger} - G_{\text{para}}^{\ddagger}$, making the corresponding $\Delta G_{\text{para}}^{\ddagger} - \Delta G_{\text{ortho}}^{\ddagger}$ value positive and thereby guaranteeing the ortho effect.

Of the total of 11 ortho-substituted iodobenzenes *o*-RC₆H₄I studied (Table 3), six (R = F, CN, Br, Cl, MeO, Me) produce OA transition states [A]TS₂ that are similar in geometry to their para-isomeric congeners. In five other cases, however (R = NO₂, CO₂Et, CHO, Ac, CO₂⁻), the O atoms of the substituents interact with the Cu center, forming chelate-like structures, as shown in Figures 9 and 10. The Cu–O bond lengths in the transition states, 2.48 Å (CO₂Et), 2.44 Å (NO₂), 2.32 Å (Ac), and 2.14 Å (CO₂⁻), vary inversely with the corresponding $\Delta G_{\text{H}}^{\ddagger} - \Delta G_{\text{ortho}}^{\ddagger}$ values (Table 3), i.e., with the ortho effect. Even a much weaker Cu···O interaction (3.04 Å > the sum of the van der Waals radii of Cu and O) found in the *o*-formyl-bearing transition state lowers its energy by 0.8 kcal/mol in comparison with the other conformer (Figure 10).

DISCUSSION

The combined experimental and computational study shows that the trifluoromethylation of aryl halides with CHF₃-derived CuCF₃ is governed by a nonradical mechanism involving Ar–X activation with Cu(I) as the rate determining step. The most intriguing mechanistic feature of the reaction of the para-substituted substrates is the abrupt change in the gradient on the Hammett plot of log(*k_R*/*k_H*) versus σ_{p} (Figure 1, top). The two excellent linear correlations, one for R = H, Me, *t*-Bu, MeO, Cl, and Br ($\rho = +0.69$) and the other for R = Cl, Br, CO₂Et, Ac, CN, and NO₂ ($\rho = +1.83$), within the same series might be an indication of two different mechanisms operating in the reaction. A nearly identical Hammett pattern was previously observed by Foà and Cassar⁴⁵ for the oxidative addition of chloroarenes ArCl to [(Ph₃P)₃Ni] and convincingly interpreted in terms of two distinct reaction pathways. It was proposed⁴⁵ that for electron-donating and weak electron-withdrawing substituents ($\sigma \leq +0.23$), a three-center concerted oxidative addition ($\rho \approx 0$) was operational, whereas for the stronger electron-withdrawing groups with $\sigma \geq +0.23$, S_NAr ($\rho = +8.8$) governed the transformation. Is this also the case with the reactions in the current study?⁵⁶

The ρ values reported in the literature^{5j,16,37–44,53} for various copper-mediated aromatic substitution reactions span a narrow range of +0.1 to +1.1. The lower ρ value of +0.69 shown in Figure 1, top, is within this range. In contrast, the higher ρ of +1.83 is unprecedented for this type of transformations and might deal with an increase of electron density on the Cu(I) center, induced by the CF₃ ligand.⁵⁷ On the other hand, $\rho = +1.83$ is too low a value for a reaction proceeding via a Meisenheimer intermediate.⁶⁰ For instance, $\rho = +7.55$ and +8.68 at 50 °C have been reported⁶¹ for the methanolysis of para-substituted fluoro- and chlorobenzenes. Furthermore, vastly different ρ values of +6.6 and +0.61 have been obtained³⁸ for the phenoxylation reaction of a series of substituted bromoarenes with PhOK in PhOH–pyridine at 170 °C in the absence and in the presence of a Cu(I) catalyst, respectively.

In contrast with Hammett's σ_{p} , the resonance parameter σ_{p}^- correlates linearly with the entire set of log(*k_R*/*k_H*) obtained for all of the *p*-RC₆H₄I used in the study (Figure 1, bottom). The ρ

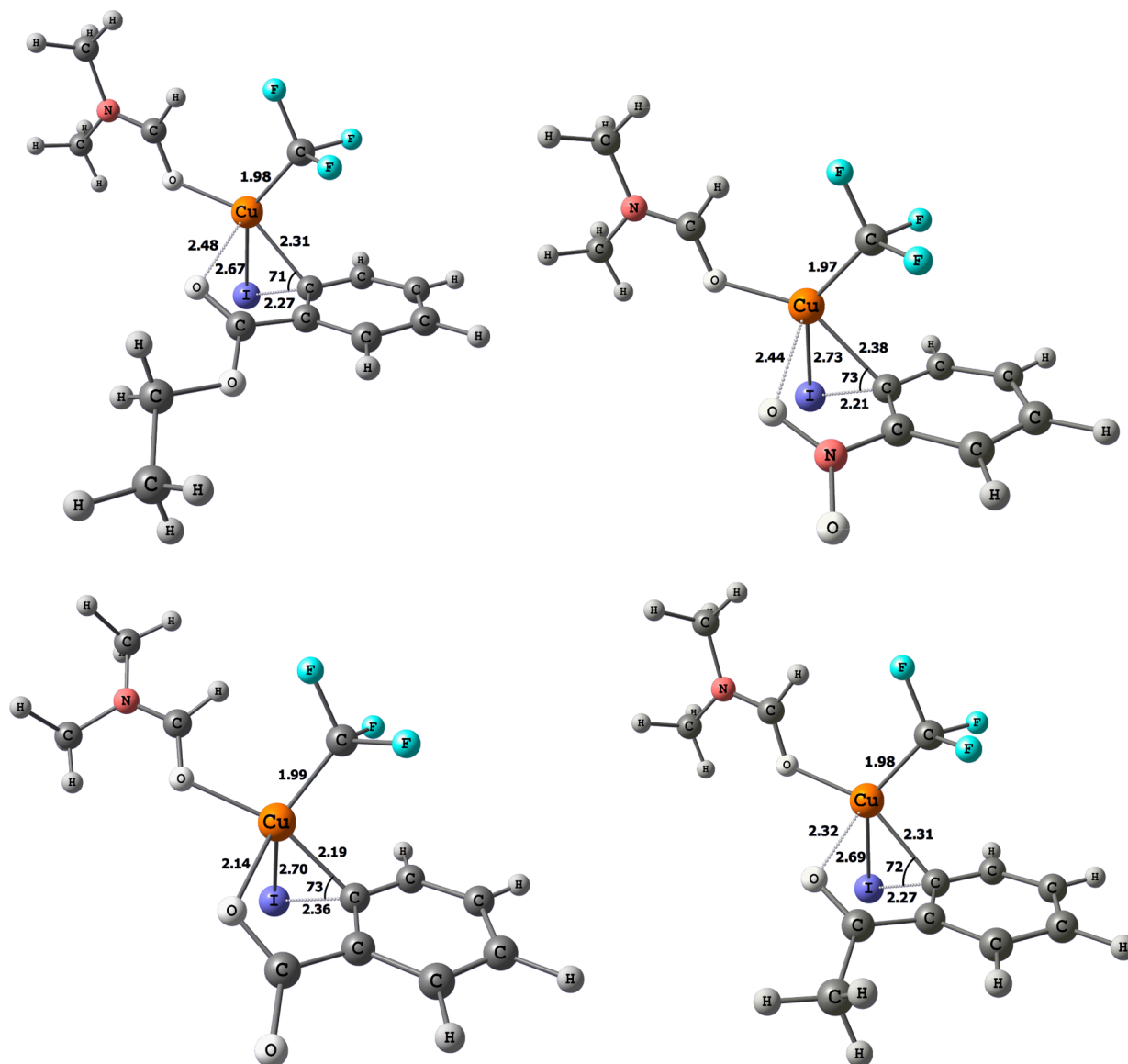


Figure 9. Computed AOARE transition states of *o*-RC₆H₄I OA to [(DMF)CuCF₃] for R = CO₂Et, NO₂, Ac, and CO₂⁻ (clockwise from upper left).

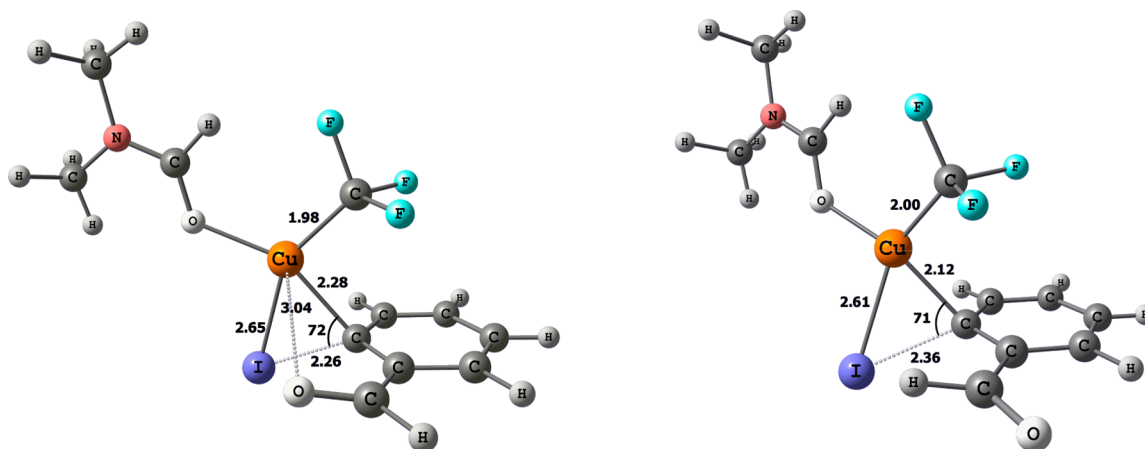


Figure 10. Computed AOARE transition states of *o*-IC₆H₄CHO OA to [(DMF)CuCF₃] with (left) and without (right) chelation.

value of +0.91 derived from the plot falls in the aforementioned range of +0.1 to +1.1 that is characteristic of Cu-mediated coupling reactions of aryl halides. This linear correlation with the

resonance parameter σ_p^- is excellent ($R^2 = 0.99$), suggesting that the transformation is governed by only one rather than two mechanisms and that there is substantial mesomeric interaction

Table 4. Computed (MM and DFT) Energy Parameters for *o*- and *p*-RC₆H₄I

R	$G^{\circ}_{\text{ortho}} - G^{\circ}_{\text{para}}$ kcal/mol (DFT) ^a	$E^{\circ}_{\text{ortho}} - E^{\circ}_{\text{para}}$ kcal/mol (MM)	contributions to strain, %			
			van der Waals	stretching	bending	torsion
Me	1.1	1.4	64	18	18	
CN	0.8	1.2	70	13	17	
MeO	0.6	0.7	83	21	-4	
F	0.5	0.3	82	12	6	
Cl	1.9	1.4	70	12	18	
Br	2.1	1.7	67	12	21	
CHO	2.8	2.5	60	17	23	
Ac	5.1	4.9	10	5	12	73
CO ₂ Et	4.5	4.7	21	8	22	49
NO ₂	5.4	4.4	5	4	11	80
CO ₂ ⁻	2.5	4.8	29	10	24	37

^aFrom Table 3.

between a -M substituent on the ring and the reaction center in the transition state for the rate determining step.³⁶

Given the above, the question remains whether one or two mechanisms are operational in the trifluoromethylation reaction of haloarenes with the CuCF₃ depending on the nature of the substrate. While without additional information this point would be moot, our computational results provide a fairly straightforward answer to this question.

The computational data suggest that S_NAr as well as SBM, SET (both outer and inner sphere), and HAT mechanisms are prohibitively high in energy. For PhI, both oxidative addition-reductive elimination mechanisms, dissociative (DOARE, $\Delta G^{\ddagger} = 24.6$ kcal/mol) and associative (AOARE, $\Delta G^{\ddagger} = 21.9$ kcal/mol), display computed barriers that are in good agreement with the estimated experimental value $\Delta G^{\ddagger} = 24$ kcal/mol at 298 K (see the Supporting Information). However, DOARE predicts that electron-enriched iodoarenes should undergo the trifluoromethylation faster than more electron-deficient ones, which is in contradiction with the experimentally observed trend. On the contrary, the AOARE pathway is delightfully consistent with the experimental data obtained in all of the Hammett and ortho effect studies.

The AOARE mechanism (Figure 4) shows no signs of a Meisenheimer-type intermediate involved in the reaction. Highly informative intimate details of the AOARE process are revealed by the structure of the OA transition state [A]TS₁. Although care should be exercised when comparing intermediates and transition states, it might be useful, in this particular case, to juxtapose [A]TS₁ with structurally characterized Meisenheimer complexes.⁶² The benzene ring in Meisenheimer intermediates conventionally adopts a sofa conformation, and a roughly tetrahedral geometry is observed at the sp³-hybridized ipso carbon. In contrast, for all of the substrates studied in the current work, the benzene ring in [A]TS₁ (Figure 6) shows virtually no deviation from planarity, with the C-C-C ipso angle varying in a narrow range of 121–122°. The nitro group in the *p*-NO₂C₆H₄I-derived [A]TS₁ is coplanar with the benzene ring, showing a noticeable contraction of the C-N bond (1.45 Å) as compared to the experimentally determined (1.472(3) Å)⁶³ and computed (1.47 Å) values for the reactant. This is a clear indication that, in the transition state, the NO₂ group is involved in an enhanced conjugative interaction with the π -system of the benzene ring. A crude yet informative estimate of the magnitude of π -conjugation in [A]TS₁ can be obtained from some reported structural data. The C-N bond distance of 1.45 Å in [A]TS₁ for *p*-NO₂C₆H₄I is longer than in the Meisenheimer complexes⁶²

and Domenicano's classical quinoid-like structure of *p*-nitroaniline (1.434(2) Å),^{64,65} yet comparable to that in *p*-nitroanisole (1.450(6) Å)⁶⁶ with substantial cross-conjugation of the MeO (+M) and NO₂ (-M) groups. The reaction center in [A]TS₁ is therefore undoubtedly influenced by resonance effects of substituents R on the ring, i.e., exactly the case where σ_p^- rather than σ_p should be used for Hammett-type correlations.³⁶ As there cannot be resonance interactions between the ipso carbon and R in the meta position, the excellent linear correlation with σ_m for the *m*-RC₆H₄I series (Figure 2) observed experimentally and computationally provides additional evidence for the AOARE pathway with [A]TS₁ as the key transition state.

All of the above points to the trifluoromethylation of aryl halides with CuCF₃ being governed by a mechanism involving OA of the Ar-X bond to the Cu(I) center as the rate determining step, followed by Ar-CF₃ reductive elimination from the resultant Cu(III) intermediate. Since the original work of Cohen⁶⁷ in the mid-1970s, the Cu(I)/Cu(III) mechanism for Cu-mediated/catalyzed reactions of haloarenes has received substantial support, especially in recent years.^{33b-f,68-71} For all 18 para- and meta-substituted iodobenzenes used in the current work, the found [A]TS₁ structures are all very much alike, displaying no signs of variation in the reaction mechanism. This also applies to the ortho-substituted substrates, which nonetheless should and will be considered separately in order to analyze and discuss the ortho effect.

There are two ways to define the ortho effect. One definition is the enhanced reactivity of an ortho-substituted haloarene in comparison with its unsubstituted phenyl halide analogue, i.e., $\Delta G^{\ddagger}_{\text{H}} - \Delta G^{\ddagger}_{\text{ortho}}$ (Tables 2 and 3). In this case, the contributions from the steric and electronic factors to the ortho effect would be particularly difficult to compare as the electronic effects of the substituent R may appear vastly different from those of the hydrogen atom. Alternatively, reaction rates of the ortho vs meta or para isomers could be compared to quantify the ortho effect as the difference in activation barriers $\Delta G^{\ddagger}_{\text{meta}} - \Delta G^{\ddagger}_{\text{ortho}}$ or $\Delta G^{\ddagger}_{\text{para}} - \Delta G^{\ddagger}_{\text{ortho}}$ (Table 3), respectively. In these cases, the same substituent possessing certain electronic properties is present on the benzene ring of both substrates, albeit in different positions. Use of $\Delta G^{\ddagger}_{\text{meta}} - \Delta G^{\ddagger}_{\text{ortho}}$ is less preferred because resonance effects of the substituent are not transmitted from the meta position. Moving the group from the para to the ortho position within the ring, however, might also result in a partial or full loss of the conjugation from the sterics forcing the substituent out of the plane. In addition, inductive effects are more efficiently transmitted from the more proximal ortho rather than from the

meta or para positions. Clearly, separating and quantifying steric and electronic contributions to the overall ortho effect is nontrivial, especially by solely experimental means. However, the reactions under study are very weakly sensitive to electronic effects of the substituents in general, as follows from the low ρ values determined both experimentally and confirmed computationally. Furthermore, steric factors have a much greater impact on the rate, as follows from a number of experimental observations. For instance, the introduction of a weakly *electron-donating* methyl group into an ortho position of bromobenzene results in a 3.5-fold increase in the reaction rate of the *nucleophilic* trifluoromethylation. In line with this, iodobenzene is only ca. 20 times less reactive toward CuCF_3 than *p*-nitroiodobenzene, whereas *o*-nitroiodobenzene reacts 4300 times faster than bromobenzene. It is therefore justified to focus mainly on steric and coordination factors contributing to the ortho effect.

In terms of $\Delta G_{\text{para}}^{\ddagger} - \Delta G_{\text{ortho}}^{\ddagger}$, the ortho effect is a sum of two additives, the difference in the ground free energies of the ortho and para isomers of the substrate $G_{\text{ortho}}^{\circ} - G_{\text{para}}^{\circ}$ and the energy difference between the corresponding transition states $G_{\text{ortho}}^{\ddagger} - G_{\text{para}}^{\ddagger}$. As established previously⁵⁵ and confirmed in the current study, a 1,2-disubstituted benzene always lies higher in energy than its 1,4-isomer. To gain insight into the factors contributing to the lower stability of ortho isomers, we performed molecular mechanics (MM) calculations using the UFF method for the ortho and para isomeric substrates studied in the current work. As can be seen from Table 4, the trend observed in the DFT studies is well-reproduced in the MM-derived $E_{\text{ortho}}^{\circ} - E_{\text{para}}^{\circ}$ values. Depending on the size and the structure of the ortho substituent, the strain imposed on the molecule varies in both the magnitude and contributions from such interactions as van der Waals repulsions, stretching, bending, and twisting about the C–R single bond (torsional effects). For the monatomic (F, Cl, Br) and smaller groups (CN, Me, MeO, CHO), the van der Waals repulsion is the main source of the strain (ca. 60–85%) with the stretching (ca. 12–21%) and bending (–4–23%) contributing less, albeit noticeably. These effects raise the energy of the ortho versus para isomer ($E_{\text{ortho}}^{\circ} - E_{\text{para}}^{\circ}$) by 0.3 kcal/mol (F) to 2.5 kcal/mol (CHO), ultimately resulting in the weak to moderate ortho effect. The bulkiest groups, Ac, CO_2Et , and NO_2 that are coplanar with the benzene ring when in the para position are twisted in the ortho isomers (Table 5; see also Figures 9 and 10)

Table 5. Computed (MM and DFT) Dihedral Angles between the Planes of the Benzene Ring and R in $\text{RC}_6\text{H}_4\text{I}$

R	DFT	MM
<i>ortho</i> - CO_2Et	40	29
<i>para</i> - CO_2Et	0	0
<i>ortho</i> - NO_2	42	41
<i>para</i> - NO_2	0	0
<i>ortho</i> -Ac	31	36
<i>para</i> -Ac	0	0
<i>ortho</i> - CO_2^-	82	25
<i>para</i> - CO_2^-	2	0

to alleviate the repulsion from the neighboring halogen atom. Accordingly, the torsion effect becomes the largest contributor (ca. 50–80%) to the overall strain, with the biggest $E_{\text{ortho}}^{\circ} - E_{\text{para}}^{\circ}$ difference observed (4.4–4.9 kcal/mol). Note that the smaller formyl group is coplanar with the aromatic ring for both orientations toward the iodine atom.

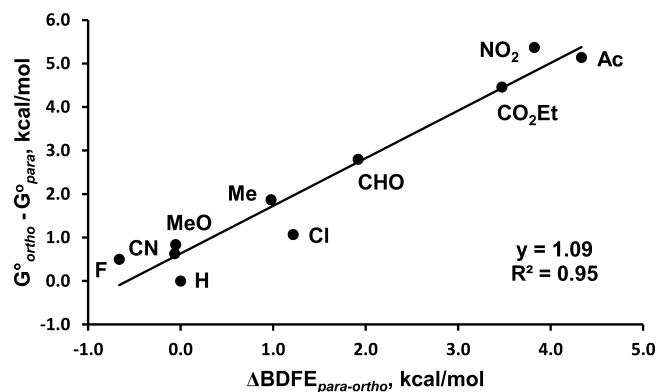


Figure 11. Plot of $G_{\text{ortho}}^{\circ} - G_{\text{para}}^{\circ}$ vs C–I $\Delta\text{BDFE}_{\text{para-ortho}}$ computed for ortho and para isomers of $\text{RC}_6\text{H}_4\text{I}$.

The strain accumulated in the ground state of the aryl halide results in the weakening of the carbon–halogen bond, as follows from Figure 11 showing correlation between $G_{\text{ortho}}^{\circ} - G_{\text{para}}^{\circ}$ and the difference in C–I bond dissociation free energy $\Delta\text{BDFE}_{\text{para-ortho}}$ computed for the same series of the ortho and para isomers of $\text{RC}_6\text{H}_4\text{I}$. The factors causing the molecular strain in the ground state (Table 4) are likely preserved, with a certain degree of fidelity, in the OA transition state since the latter does not exhibit significant additional distortions within the aromatic moiety. This hypothesis receives support from the plot in Figure 12 showing that $\Delta G_{\text{para}}^{\ddagger} - \Delta G_{\text{ortho}}^{\ddagger}$ (ortho effect) vary directly with C–I $\Delta\text{BDFE}_{\text{para-ortho}}$.

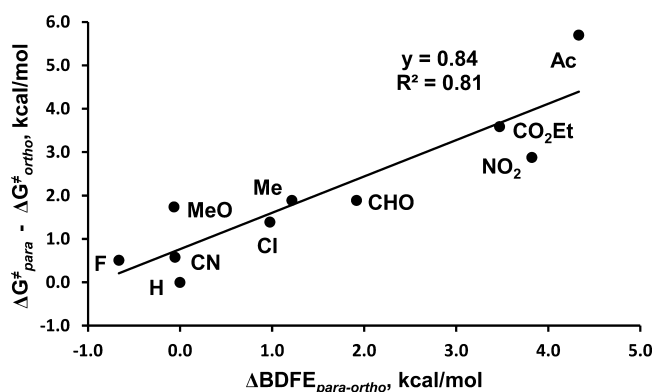


Figure 12. Plot of $\Delta G_{\text{para}}^{\ddagger} - \Delta G_{\text{ortho}}^{\ddagger}$ (ortho effect) vs C–I $\Delta\text{BDFE}_{\text{para-ortho}}$ computed for the activation barriers of OA of *o*- $\text{RC}_6\text{H}_4\text{I}$ and *p*- $\text{RC}_6\text{H}_4\text{I}$ to $[(\text{DMF})\text{CuCF}_3]$.

The above shows that, apart from the evidently minor contributions of electronic factors, the ortho effect is largely determined by two parameters. One is the effective steric bulk of the ortho substituent that raises the innate free energy of the substrate by introducing molecular strain and, as a result, weakening the bond to be broken in the rate determining step of the reaction. The other factor deals with the ability of the functional group in the ortho position to interact with the metal center in the transition state, thereby stabilizing it and consequently lowering the overall barrier to the transformation. The strength of this coordination for $\text{R} = \text{CHO}, \text{CO}_2\text{Et}, \text{NO}_2, \text{Ac}$, and CO_2^- ultimately translating into the ortho effect varies in a broad range and may be quantified by the Cu–O distance in the transition state. As discussed above, the magnitude of the ortho effect in terms of the $\Delta G_{\text{H}}^{\ddagger} - \Delta G_{\text{ortho}}^{\ddagger}$ or $\Delta G_{\text{para}}^{\ddagger} - \Delta G_{\text{ortho}}^{\ddagger}$

values (Table 3) correlates with the strength of the Cu...O interaction, i.e., inversely with the distance between the two atoms: CHO (3.04 Å) < CO₂Et (2.48 Å) < NO₂ (2.44 Å) < Ac (2.32 Å) < CO₂⁻ (2.14 Å).

In the discussion above, the carboxyl group prompting by far the strongest ortho-effect is somewhat set aside from, and not as frequently included in the quantitative comparisons as, CHO, CO₂Et, NO₂, and Ac. This was done intentionally because, unlike in the case of all other ortho substituents in the current study, efficient coordination of the carboxyl to the Cu center involves O–H ionization. Consequently, the *ortho*-halobenzoic acid substrates were modeled in the current work as the corresponding carboxylate anions. Proton transfer from the carboxyl is not expected to be energetically demanding under the experimentally used conditions, particularly in the presence of Et₃N (see above). However, for the sake of consistency of the data, the acid–base equilibria involved in the trifluoromethylation of *o*-halobenzoic acids were excluded from consideration in the computational studies. This simplification neither influences any of the conclusions nor alters the new level of understanding of the ortho effect reached in the current study.

SUMMARY AND CONCLUSIONS

The trifluoromethylation reaction of a variety of aryl halides with fluoroform-derived CuCF₃ has been studied by experimental (radical clock, kinetic, Hammett correlation) and computational (DFT, MM) means. The combined data set points to a bimolecular process involving Ar–X oxidative addition to DMF-stabilized CuCF₃ as the rate determining step, followed by Ar–CF₃ reductive elimination from a Cu(III) intermediate. The computed barrier for the trifluoromethylation of iodobenzene ($\Delta G^\ddagger = 21.9$ kcal/mol at 298 K) is in good agreement with the experimental value of $\Delta G^\ddagger = 24$ kcal/mol at 298 K. A radical mechanism has been ruled out on the basis of both experimental and computational data. The latter have also shown prohibitively high barriers to SET (both outer and inner sphere) as well as classical S_NAr, SBM, and HAT processes previously proposed in the literature for some other Cu-mediated coupling reactions of aryl halides. Most remarkably, the DFT calculations have successfully reproduced the striking results of the experimental Hammett studies.

The Ar–CF₃ bond forming reaction of ArX with CuCF₃ is weakly sensitive to substituents in the para and meta positions of the aromatic ring. The Hammett study of a series of 8 meta-substituted iodoarenes *m*-RC₆H₄I (R = H, Me, MeO, CO₂Et, CHO, Cl, CN, and NO₂) has produced an excellent linear correlation between $\log(k_R/k_H)$ and σ_m ($\rho = +0.97$). Most unexpectedly, however, a sharp change in the gradient has been observed on the Hammett plot of $\log(k_R/k_H)$ versus σ_p for a series of 11 para-substituted iodoarenes. Two linear correlations with σ_p , one for R = H, Me, *t*-Bu, MeO, Cl, and Br ($\rho = +0.69$) and the other for R = F, Cl, Br, CO₂Et, Ac, CN, and NO₂ ($\rho = +1.83$), could be generated within the same series (Figure 1, top). While we are unaware of such Hammett dualism reported for Cu-catalyzed/promoted coupling reactions, a strikingly similar effect has been observed by Foà and Cassar for the oxidative addition of substituted chlorobenzenes to [(Ph₃P)₃Ni].⁴⁵ In that report, the two linear Hammett plots within the same series of substrates were convincingly interpreted in terms of two distinct reaction mechanisms, a three-center concerted oxidative addition ($\rho \approx 0$) for electron-donating and weak electron-withdrawing substituents, and S_NAr ($\rho = +8.8$) for stronger electron-acceptors with $\sigma > +0.23$. As tempting as it could be to rationalize the current

results in a similar way, an in-depth analysis of the data suggests that, regardless of the nature and position of a substituent on the ring, there is only one reaction pathway for the transformation. For solving the mysterious “one or two mechanisms” dilemma, it has been critical to find a single linear correlation ($\rho = +0.91$; $R^2 = 0.99$) of the entire set of $\log(k_R/k_H)$ with the resonance parameter σ_p^- in place of σ_p (Figure 1, bottom). Indicative of only one mechanism with considerable resonance interaction between the reaction center and the substituent, this interpretation has received strong support from (i) comparative analysis of the experimental ρ values; (ii) unambiguous signs of enhanced –M effects of the substituent in the transition state for the Ar–I oxidative addition; (iii) close similarity of the transition states regardless of substituents in the meta or para positions; and (iv) remarkably faithful reproduction of the Hammett plot by the DFT data.

We have also performed the first detailed study of the ortho effect, a long-known and broadly used in synthesis, yet poorly understood phenomenon of the enhanced reactivity of ortho-substituted aryl halides in Cu-mediated/catalyzed coupling reactions. In the current work, the ortho effect has been quantified, for the first time, for the reaction of CuCF₃ with a series of *o*-RC₆H₄Br using the competitive kinetics method to produce the following relative rate constants k_R/k_H : H (1) < Me (3.5) < MeO (4) < CN (20) < CHO (250) < CO₂Me (850) < NO₂ (4300) < Ac (7300) < CO₂H (150 000). This order of reactivity determined experimentally and reproduced by DFT calculations cannot be rationalized solely in terms of chelation as has been proposed previously. The positive ρ values obtained by us and reported by others for a variety of Cu-mediated reactions of haloarenes suggest that electron donation from the methyl and methoxy groups in the ortho position should slow down the reaction. In fact, the opposite is observed experimentally, pointing to the minor role of electronic factors in the ortho effect. Similarly, *p*-nitroiodobenzene is only ca. 20 times more reactive than iodobenzene, whereas *o*-nitroiodobenzene reacts 4300 faster than bromobenzene.

The ortho effect is largely determined by two parameters. One is the chelation proposed in some previous reports, albeit without any evidence. Coordination of an ortho substituent to the Cu center stabilizes the transition state for the Ar–X oxidative addition, thus lowering the overall barrier for the transformation. The efficacy of the Cu...O interaction measured as the computed distance between the two atoms for CHO (3.04 Å) > CO₂Et (2.48 Å) > NO₂ (2.44 Å) > Ac (2.32 Å) > CO₂⁻ (2.14 Å) determines the magnitude of the ortho effect in terms of the $\Delta G^\ddagger_H - \Delta G^\ddagger_{ortho}$ or $\Delta G^\ddagger_{para} - \Delta G^\ddagger_{ortho}$ values. There is, however, another key contributor to the ortho effect. The steric bulk of the *o*-substituent raises the ground state free energy of the haloarene ($G^\circ_{ortho} - G^\circ_{para}$ or $G^\circ_{ortho} - G^\circ_H$) by introducing molecular strain and consequently weakening the Ar–X bond to be broken in the rate determining step. Apart from the rather insignificant electronic effects (see above), this ground state energy factor is apparently the only one bringing about the ortho effect in the case of nonchelating groups, such as Me, MeO, CN, Cl, Br, etc.

The experimental and computational results obtained in this work shed light on the mechanism of the highly important trifluoromethylation of aryl halides with CuCF₃. Furthermore, the studies performed in the current work take us to the next level of understanding of the ortho effect in the chemistry of Cu-catalyzed/mediated coupling reactions of aryl halides. It is hoped that the deeper mechanistic insights stemming from the current

study will be useful for further advances in both basic and applied research.

EXPERIMENTAL SECTION

All chemicals, solvents, and deuterated solvents were purchased from Aldrich, Alfa Aesar, Apollo Scientific, TCI, and Acros chemical companies. Anhydrous DMF (Alfa Aesar or from an MBraun SPS) and acetonitrile (distilled from P_2O_5 under argon) were stored over freshly calcined 4 Å molecular sieves in a glovebox. Fluoroform-derived $CuCF_3$ was prepared in DMF and stabilized with $Et_3N \cdot 3HF$ ($1/3$ mol per mol $CuCF_3$), as reported previously.^{20a} A literature procedure⁷² was used to synthesize 1-allyloxy-2-iodobenzene. NMR spectra were recorded on a Bruker Avance 400 Ultrashield spectrometer at 25 °C. Quantitative ^{19}F NMR analyses were carried out with $D1 = 5$ s. An Agilent Technologies 7890A chromatograph equipped with a 5975C MSD unit was used for GC–MS analysis.

Reaction of $CuCF_3$ with 1-Allyloxy-2-iodobenzene (Radical Clock). In a glovebox, the $CuCF_3$ reagent in DMF (0.38 M, 0.6 mL, 0.23 mmol) was added to a mixture of 4,4'-difluorobiphenyl (internal standard, 16 mg, 0.08 mmol) and 1-allyloxy-2-iodobenzene (296 mg, 1.14 mmol). The resultant solution was sealed in an NMR tube, brought out, and kept at room temperature for 1 day. Quantitative ^{19}F NMR analysis indicated the formation of 1-allyloxy-2-(trifluoromethyl)benzene^{5c} in 60% yield ($\delta = -61.4$ ppm, singlet) at 70% conversion of the $CuCF_3$. No cyclized product^{2b} was detected in the reaction solution (^{19}F NMR, GC–MS).

Determination of Reaction Orders by the Method of Initial Rates. All reactions were run to 10–20% conversion. For specifics, see Supporting Information Table S1. For experiments with liquid aryl halides, 4,4'-difluorobiphenyl (internal standard, 16 mg, 0.08 mmol) was weighed into a 5 mm glass NMR tube in air. The NMR tube was brought to an argon-filled glovebox and charged with $CuCF_3$ in DMF (0.38 M) or with $CuCF_3$ in DMF (0.38 M) and pure DMF or MeCN or both for dilution. The total volume of the solution was 0.6 mL in all cases. The tube was sealed with a rubber septum and brought out. A liquid haloarene was added via microsyringe (Supporting Information Table S1), and kinetic measurements on the sample by ^{19}F NMR were started immediately. For experiments with solid aryl halides, a haloarene and the internal standard, 4,4'-difluorobiphenyl (16 mg, 0.08 mmol), were weighed into a 5 mm glass NMR tube in air. The tube was brought to an argon-filled glovebox and either sealed with a rubber septum and brought out, or first charged with DMF, or MeCN, or both (Supporting Information Table S1) and then sealed and brought out. ^{19}F NMR quantitative measurements on the sample were commenced immediately after a solution of $CuCF_3$ in DMF (0.38 M) was syringed in.

Determination of k_R/k_H for Para- and Meta-Substituted Aryl Iodides. See Supporting Information Table S2 for specifics. In an argon-filled glovebox, the $CuCF_3$ reagent in DMF (0.38 M, 0.1 mL, 0.04 mmol) was added to a 5 mm glass NMR tube containing a solution of PhI (43 μ L, 0.38 mmol) and an aryl iodide (0.38 mmol) in DMF (0.5 mL). The tube was sealed with a rubber septum and its contents were thoroughly shaken. Quantitative ^{19}F NMR analysis of the sample was performed ca. 30 min after mixing the reagents. The experiments were repeated with a mixture of MeCN (0.3 mL) and DMF (0.2 mL) in place of 5 mL of pure DMF. No significant difference in the relative reactivity was noticed. As $m-CF_3C_6H_4OMe$ and $PhCF_3$ exhibit very similar ^{19}F NMR chemical shifts, the relative reactivity of $m-IC_6H_4OMe$ was determined in a similar experiment using $m-IC_6H_4CHO$ (48 μ L, 0.38 mmol) in place of PhI. The $m-CF_3C_6H_4OMe$ to $m-CF_3C_6H_4CHO$ ratio determined in this experiment was 1:2.

Determination of k_R/k_H for Ortho-Substituted Aryl Bromides. Details for PhBr versus $o-BrC_6H_4R$ ($R = Me, MeO, CN$) follow. In a glovebox, to a solution of $o-BrC_6H_4Me$ (purity 99%, 0.23 mL, 1.85 mmol) and PhBr (purity 99%, 0.2 mL, 1.85 mmol) in DMF (0.2 mL) placed in a 5 mm glass NMR tube was added the $CuCF_3$ reagent in DMF (0.37 M, 0.5 mL, 0.19 mmol). The tube was sealed with a rubber septum, and its contents were thoroughly shaken. Quantitative ^{19}F NMR analysis of the sample was performed 24 h after mixing the reagents. The reaction mixture was diluted with ether (2 mL), washed with water (5 mL), and analyzed by ^{19}F NMR. The $PhCF_3$ (-61.7 ppm) to $o-MeC_6H_4CF_3$

(-60.6 ppm) ratio was 1:3.5. This procedure was repeated first with $o-BrC_6H_4OMe$ (purity 98%, 0.24 mL, 1.85 mmol) in place of $o-BrC_6H_4Me$ and then with $o-BrC_6H_4CN$ (purity 99%, 340 mg, 1.85 mmol) in place of $o-BrC_6H_4Me$. The $PhCF_3$ to $o-MeOC_6H_4CF_3$ (-61.3 ppm) and to $o-NCC_6H_4CF_3$ (-60.9 ppm) ratios were 1:4 and 1:20, respectively. Details for $o-BrC_6H_4CHO$ versus $o-BrC_6H_4R$ ($R = CN, CO_2Me$) follow. In a glovebox, to a solution of $o-BrC_6H_4CHO$ (purity 98%, 0.09 mL, 0.74 mmol) and $o-BrC_6H_4CN$ (136 mg, 0.74 mmol) in DMF (0.5 mL) placed in a 5 mm NMR tube was added the $CuCF_3$ reagent (0.37 M, 0.2 mL, 0.07 mmol). The tube was sealed with a rubber septum, and its contents were thoroughly shaken. Quantitative ^{19}F NMR analysis of the sample was performed 1 h after mixing the reagents. The reaction mixture was diluted with ether (2 mL), washed with saturated aqueous solution of Na_2CO_3 (5 mL), and analyzed by ^{19}F NMR. The $o-CF_3C_6H_4CN$ (-60.9 ppm) to $o-CF_3C_6H_4CHO$ (-54.7 ppm) ratio was 1:12. This procedure was repeated with $o-BrC_6H_4CO_2Me$ (purity 98%, 0.11 mL, 0.74 mmol) in place of $o-BrC_6H_4CN$. The $o-CF_3C_6H_4CHO$ to $o-CF_3C_6H_4CO_2Me$ (-58.7 ppm) ratio was 1:3.5. Details for $o-BrC_6H_4CO_2Me$ versus $o-BrC_6H_4NO_2$ follow. In a glovebox, to a solution of $o-BrC_6H_4NO_2$ (purity 98%, 76 mg, 0.37 mmol) and $o-BrC_6H_4CO_2Me$ (53 μ L, 0.37 mmol) in DMF (0.5 mL) placed in a 5 mm NMR tube was added the $CuCF_3$ reagent (0.37 M, 0.1 mL, 0.04 mmol). The tube was sealed with a rubber septum, and its contents were thoroughly shaken. Quantitative ^{19}F NMR analysis of the sample performed 30 min after mixing the reagents indicated the $o-CF_3C_6H_4CO_2Me$ (-58.7 ppm) to $o-CF_3C_6H_4NO_2$ (-59.1 ppm) ratio of 1:5. Details for $o-BrC_6H_4NO_2$ versus $o-BrC_6H_4Ac$ follow. In a glovebox, to a solution of $o-BrC_6H_4Ac$ (purity 99%, 0.1 mL, 0.74 mmol) and $o-BrC_6H_4NO_2$ (153 mg, 0.74 mmol) in DMF (0.5 mL) placed in a 5 mm NMR tube was added the $CuCF_3$ reagent (0.37 M, 0.2 mL, 0.074 mmol). The tube was sealed with a rubber septum, and its contents were thoroughly shaken. Quantitative ^{19}F NMR analysis of the sample performed 30 min after mixing the reagents indicated the $o-CF_3C_6H_4NO_2$ (-59.1 ppm) to $o-CF_3C_6H_4Ac$ (-57.3 ppm) ratio of 1:1.7. Details for $o-BrC_6H_4Ac$ versus $o-BrC_6H_4R$ ($R = CO_2H$ and NO_2) follow. In a glovebox, to a solution of $o-BrC_6H_4CO_2H$ (purity 97%, 77 mg, 0.37 mmol), $o-BrC_6H_4Ac$ (0.05 mL, 0.37 mmol), and $o-BrC_6H_4NO_2$ (76 mg, 0.37 mmol) in DMF (0.5 mL) placed in a 5 mm NMR tube was added the $CuCF_3$ reagent (0.37 M, 0.1 mL, 0.04 mmol). The tube was sealed with a rubber septum, and its contents were thoroughly shaken. Quantitative ^{19}F NMR analysis of the sample performed 10 min after mixing the reagents indicated the $o-CF_3C_6H_4NO_2$ (-59.1 ppm) to $o-CF_3C_6H_4Ac$ (-57.3 ppm) to $o-CF_3C_6H_4CO_2H$ (-58.3 ppm) ratio of 1:2.5:52. Note that the $o-CF_3C_6H_4NO_2$ (-59.1 ppm) to $o-CF_3C_6H_4Ac$ (-57.3 ppm) ratio of 1:2.5 differs slightly from that (1:1.7) determined in the experiment described above. This minor difference deals with the integration error being considerably larger than the standard value of ca. 10% for weak signals. Therefore, the more accurate 1:1.7 ratio obtained in the previous experiment ($o-BrC_6H_4NO_2$ vs $o-BrC_6H_4Ac$) was used for the order of reactivity.

Computational Details. All DFT calculations were carried out using the Gaussian suite of programs.⁷³ The geometries were fully optimized without any constraints with dispersion-corrected B3LYP-D functional⁷⁴ and ultrafine integration grid. Solvent effects were taken into account by means of the implicit polarizable continuum model (PCM) and DMF as a solvent ($\epsilon = 37.219$).⁷⁵ Copper and all halogen atoms except fluorine were described with Stuttgart RECPs and associated basis sets⁷⁶ augmented with additional polarization functions on Cl, Br, and I centers ($\zeta_d = 0.640, 0.428, \text{ and } 0.289$, respectively).⁷⁷ Standard full electron Pople's basis set 6-31+G(d) was used for all other atoms.⁷⁸ This basis set combination is denoted as BS1. All computed structures were characterized as local stationary points via analytical frequency calculations at the standard state (298.15 K, 1 atm). For saddle points, intrinsic reaction coordinate (IRC) analysis⁷⁹ with the subsequent geometry optimization was performed to verify that they are linked by the corresponding minima on the potential energy surface. Additional single-point calculations based on B3LYP-D/BS1 optimized geometries were performed with a double hybrid mPW2PLYPD functional⁸⁰ and a larger basis set combination denoted as BS2. This includes the same ECP and basis set for Cu, Cl, Br, and I with added f-

orbital polarization on Cu ($\zeta_r = 3.525$).⁸¹ For the first and second row elements, the all-electron 6-311++G(2d,p) basis set was employed.⁸² These mPW2PLYPD/BS2 energies modified by the Gibbs free energy correction from B3LYP-D/BS1 calculations were conducted to describe the reaction energies throughout the study. The UFF method as implemented in Gaussian 09 was used to perform the MM calculations.⁸³

■ ASSOCIATED CONTENT

Supporting Information

Full details of experimental and computational studies. This material is available free of charge via the Internet at <http://pubs.acs.org>.

■ AUTHOR INFORMATION

Corresponding Author

vgrushin@iciq.es

Notes

The authors declare no competing financial interest.

■ ACKNOWLEDGMENTS

We thank Feliu Maseras for very helpful discussions and valuable advice and Stuart A. Macgregor for discussions and preliminary computational data. Fedor M. Miloserdov is gratefully acknowledged for numerous thought-provoking fruitful discussions. This work was supported by the ICIQ Foundation and the Spanish Government (Grant CTQ2011-25418).

■ REFERENCES

- (1) (a) McLoughlin, V. C. R.; Thrower, J. U.S. Patent 3408411, 1968. (b) McLoughlin, V. C. R.; Thrower, J. *Tetrahedron* **1969**, *25*, 5921.
- (2) For selected monographs, see: (a) Hudlicky, M. *Chemistry of Organic Fluorine Compounds*; Ellis Horwood: New York, 1976. (b) Banks, R. E. *Organofluorine Chemicals and Their Industrial Applications*; Ellis Horwood: West Sussex, U.K., 1979. (c) Filler, R.; Kobayashi, Y. *Biomedical Aspects of Fluorine Chemistry*; Kodansha-Elsevier: New York, 1982. (d) Clark, J. H.; Wails, D.; Bastock, T. W. *Aromatic Fluorination*; CRC Press: Boca Raton, FL, 1996. (e) Kirsch, P. *Modern Fluoroorganic Chemistry*; Wiley-VCH: Weinheim, 2004. (f) Uneyama, K. *Organofluorine Chemistry*; Blackwell: Oxford, U.K., 2006. (g) Ojima, I. *Fluorine in Medicinal Chemistry and Chemical Biology*; Wiley-Blackwell: Chichester, U.K., 2009. (h) Petrov, V. A. *Fluorinated Heterocyclic Compounds. Synthesis, Chemistry and Applications*; Wiley: Hoboken, NJ, 2009.
- (3) For selected reviews, see: (a) Burton, D. J.; Yang, Z. Y. *Tetrahedron* **1992**, *48*, 189. (b) McClinton, M. A.; McClinton, D. A. *Tetrahedron* **1992**, *48*, 6555. (c) Burton, D. J.; Lu, L. *Top. Curr. Chem.* **1997**, *193*, 45. (d) Schlosser, M. *Angew. Chem., Int. Ed.* **2006**, *45*, 5432. (e) Roy, S.; Gregg, B. T.; Gribble, G. W.; Le, V.-D.; Roy, S. *Tetrahedron* **2011**, *67*, 2161. (f) Qing, F.-L.; Zheng, F. *Synlett* **2011**, 1052. (g) Liu, T.; Shen, Q. *Eur. J. Org. Chem.* **2012**, 6679. (h) Lishchynskiy, A.; Novák, P.; Grushin, V. V. In *Science of Synthesis: C-1 Building Blocks in Organic Synthesis 2*; van Leeuwen, P. W. N. M., Ed.; Thieme: Stuttgart, 2013; p 367.
- (4) For a recent comprehensive review of aromatic trifluoromethylation and perfluoroalkylation, see: Tomashenko, O. A.; Grushin, V. V. *Chem. Rev.* **2011**, *111*, 4475.
- (5) For most recent reports not covered in the review article cited in ref 4, see: (a) Zhang, C. P.; Wang, Z. L.; Chen, Q. Y.; Zhang, C. T.; Gu, Y. C.; Xiao, J. C. *Angew. Chem., Int. Ed.* **2011**, *50*, 1896. (b) Popov, L.; Lindeman, S.; Daugulis, O. *J. Am. Chem. Soc.* **2011**, *133*, 9286. (c) Morimoto, H.; Tsubogo, T.; Litvinas, N. D.; Hartwig, J. F. *Angew. Chem., Int. Ed.* **2011**, *50*, 3793. (d) Tomashenko, O. A.; Escudero-Adán, E. C.; Martínez Belmonte, M.; Grushin, V. V. *Angew. Chem., Int. Ed.* **2011**, *50*, 7655. (e) Weng, Z.; Lee, R.; Jia, W.; Yuan, Y.; Wang, W.; Feng, X.; Huang, K.-W. *Organometallics* **2011**, *30*, 3229. (f) Li, Y.; Chen, T.; Wang, H.; Zhang, R.; Jin, K.; Wang, X.; Duan, C. *Synlett* **2011**, 1713.

- (g) Kondo, H.; Oishi, M.; Fujikawa, K.; Amii, H. *Adv. Synth. Catal.* **2011**, *353*, 1247. (h) Kremlev, M. M.; Mushta, A. I.; Tyrta, W.; Yagupolskii, Y. L.; Naumann, D.; Möller, A. *J. Fluorine Chem.* **2012**, *133*, 67. (i) Sanhueza, I. A.; Nielsen, M. C.; Ottiger, M.; Schoenebeck, F. *Helv. Chim. Acta* **2012**, *95*, 2231. (j) Chen, M.; Buchwald, S. L. *Angew. Chem., Int. Ed.* **2013**, *52*, 11628. (k) Serizawa, H.; Aikawa, K.; Mikami, K. *Chem.—Eur. J.* **2013**, *19*, 17692. (l) Mulder, J. A.; Frutos, R. P.; Patel, N. D.; Qu, B.; Sun, X.; Tampone, T. G.; Gao, J.; Sarvestani, M.; Eriksson, M. C.; Haddad, N.; Shen, S.; Song, J. J.; Senanayake, C. H. *Org. Process Res. Dev.* **2013**, *17*, 940. (m) Nakamura, Y.; Fujii, M.; Murase, T.; Itoh, Y.; Serizawa, H.; Aikawa, K.; Mikami, K. *Beilstein J. Org. Chem.* **2013**, *9*, 2404. (n) Mormino, M. G.; Fier, P. S.; Hartwig, J. F. *Org. Lett.* **2014**, *16*, 1744. (o) Serizawa, H.; Aikawa, K.; Mikami, K. *Org. Lett.* **2014**, *16*, 3456. (p) Gonda, Z.; Kovács, S.; Wéber, C.; Gáti, T.; Mészáros, A.; Kotschy, A.; Novák, Z. *Org. Lett.* **2014**, *16*, 4268.

(6) For the original reports on Cu-catalyzed trifluoromethylation of aryl halides (iodides), see: (a) Oishi, M.; Kondo, H.; Amii, H. *Chem. Commun.* **2009**, 1909. (b) Inoue, M.; Araki, K. Japan Patent JP 2009-234921, 2009.

(7) (a) Kobayashi, Y.; Kumadaki, I. *Tetrahedron Lett.* **1969**, 4095. (b) For a recent account of Kumadaki's work, see: Sato, K.; Tarui, A.; Omote, M.; Ando, A.; Kumadaki, I. *Synthesis* **2010**, 1865.

(8) Kondratenko, N. V.; Vechirko, E. P.; Yagupolskii, L. M. *Synthesis* **1980**, 932.

(9) Matsui, K.; Tobita, E.; Ando, M.; Kondo, K. *Chem. Lett.* **1981**, 1719.

(10) (a) Wiemers, D. M.; Burton, D. J. *J. Am. Chem. Soc.* **1986**, *108*, 832. (b) MacNeil, J. G.; Burton, D. J. *J. Fluorine Chem.* **1991**, *55*, 225.

(11) (a) Chen, Q.-Y.; Wu, S.-W. *J. Chem. Soc., Chem. Commun.* **1989**, 705. (b) Chen, Q.-Y.; Wu, S.-W. *J. Chem. Soc., Perkin Trans. 1* **1989**, 2385. (c) Chen, Q.-Y.; Duan, J.-X. *J. Chem. Soc., Chem. Commun.* **1993**, 1389. (d) Long, Z.-Y.; Duan, J.-X.; Lin, Y.-B.; Guo, C.-Y.; Chen, Q.-Y. *J. Fluorine Chem.* **1996**, *78*, 177.

(12) Chen, G. J.; Tamborski, C. J. *Fluorine Chem.* **1989**, *43*, 207.

(13) Urata, H.; Fuchikami, T. *Tetrahedron Lett.* **1991**, *32*, 91.

(14) (a) Kuett, A.; Movchun, V.; Rodima, T.; Dansauer, T.; Rusanov, E. B.; Leito, I.; Kaljurand, I.; Koppel, J.; Pihl, V.; Koppel, I.; Ovsjannikov, G.; Toom, L.; Mishima, M.; Medebielle, M.; Lork, E.; Röschenhaler, G.-V.; Koppel, I. A.; Kolomeitsev, A. A. *J. Org. Chem.* **2008**, *73*, 2607. (b) Kremlev, M. M.; Tyrta, W.; Mushta, A. I.; Naumann, D.; Yagupolskii, Y. L. *J. Fluorine Chem.* **2010**, *131*, 212.

(15) (a) Dubinina, G. G.; Furutachi, H.; Vivic, D. A. *J. Am. Chem. Soc.* **2008**, *130*, 8600. (b) Dubinina, G. G.; Ogikubo, J.; Vivic, D. A. *Organometallics* **2008**, *27*, 6233.

(16) Carr, G. E.; Chambers, R. D.; Holmes, T. F. *J. Chem. Soc., Perkin Trans. 1* **1988**, 921.

(17) For selected reviews, see: (a) Hassan, J.; Seignion, M.; Gozzi, C.; Schulz, E.; Lemaire, M. *Chem. Rev.* **2002**, *102*, 1359. (b) Ley, S.; Thomas, A. W. *Angew. Chem., Int. Ed.* **2003**, *42*, 5400. (c) Beletskaya, I. P.; Cheprakov, A. V. *Coord. Chem. Rev.* **2004**, *248*, 2337. (d) Evano, G.; Blanchard, N.; Toumi, M. *Chem. Rev.* **2008**, *108*, 3054. (e) Monnier, F.; Taillefer, M. *Angew. Chem., Int. Ed.* **2009**, *48*, 6954. (f) Rao, H.; Fu, H. *Synlett* **2011**, 745. (g) *Copper-Mediated Cross-Coupling Reactions*; Evano, G.; Blanchard, N., Eds.; John Wiley & Sons: Hoboken, NJ, 2014.

(18) For most recent critical reviews of mechanisms of Cu-mediated/catalyzed coupling reactions of aryl halides, see: (a) Beletskaya, I. P.; Cheprakov, A. V. *Organometallics* **2012**, *31*, 7753. (b) Lefevre, G.; Franc, G.; Tlili, A.; Adamo, C.; Taillefer, M.; Ciofini, I.; Jutand, A. *Organometallics* **2012**, *31*, 7694. (c) Sperotto, E.; van Klink, G. P. M.; van Koten, G.; de Vries, J. G. *Dalton Trans.* **2010**, *39*, 10338.

(19) (a) Jones, G. O.; Liu, P.; Houk, K. N.; Buchwald, S. L. *J. Am. Chem. Soc.* **2010**, *132*, 6205. (b) Yu, H.-Z.; Jiang, Y.-Y.; Fu, Y.; Liu, L. *J. Am. Chem. Soc.* **2010**, *132*, 18078.

(20) (a) Zanardi, A.; Novikov, M. A.; Martin, E.; Benet-Buchholz, J.; Grushin, V. V. *J. Am. Chem. Soc.* **2011**, *133*, 20901. (b) Mazloomi, Z.; Bansode, A.; Benavente, P.; Lishchynskiy, A.; Urakawa, A.; Grushin, V. V. *Org. Process Res. Dev.* **2014**, *18*, 1020.

(21) Grushin, V. V. *Chim. Oggi* **2014**, *32*, 81.

(22) Kononov, A. I.; Benet-Buchholz, J.; Martin, E.; Grushin, V. V. *Angew. Chem., Int. Ed.* **2013**, *52*, 11637.

- (23) Novák, P.; Lishchynskiy, A.; Grushin, V. V. *Angew. Chem., Int. Ed.* **2012**, *51*, 7767.
- (24) Novák, P.; Lishchynskiy, A.; Grushin, V. V. *J. Am. Chem. Soc.* **2012**, *134*, 16167.
- (25) Lishchynskiy, A.; Novikov, M. A.; Martin, E.; Escudero-Adán, E. C.; Novák, P.; Grushin, V. V. *J. Org. Chem.* **2013**, *78*, 11126.
- (26) Lishchynskiy, A.; Berthon, G.; Grushin, V. V. *Chem. Commun.* **2014**, *50*, 10237.
- (27) For related transformations involving C_2F_5H -derived Cu_2F_5 , see: Lishchynskiy, A.; Grushin, V. V. *J. Am. Chem. Soc.* **2013**, *135*, 12584.
- (28) (a) Bunnett, J. F. *Acc. Chem. Res.* **1978**, *11*, 413. (b) Rossi, R. A.; de Rossi, R. H. *Aromatic Substitution by the $S_{RN}1$ Mechanism*; American Chemical Society: Washington, DC, 1983. (c) Bowman, W. R.; Heaney, H.; Smith, P. H. G. *Tetrahedron Lett.* **1984**, *25*, 5821. (d) van Leeuwen, M.; McKillop, A. J. *Chem. Soc., Perkin Trans. 1* **1993**, 2433.
- (29) Giese, B.; Kopping, B.; Göbel, T.; Dickhaut, J.; Thoma, G.; Kulicke, K. J.; Trach, F. *Org. React.* **1996**, *48*, 301.
- (30) (a) Johnston, L. J.; Lusztlyk, J.; Wayner, D. D. M.; Abeywickreya, A. N.; Beckwith, A. L. J.; Scaiano, J. C.; Ingold, K. U. *J. Am. Chem. Soc.* **1985**, *107*, 4594. (b) Abeywickreya, A. N.; Beckwith, A. L. J. *Chem. Commun.* **1986**, 464. (c) Abeywickreya, A. N.; Beckwith, A. L. J.; Gerba, S. J. *Org. Chem.* **1987**, *52*, 4072. (d) Annunziata, A.; Galli, C.; Marinelli, M.; Pau, T. *Eur. J. Org. Chem.* **2001**, 1323.
- (31) (a) Creutz, S. E.; Lotito, K. J.; Fu, G. C.; Peters, J. C. *Science* **2012**, *338*, 647. (b) Uyeda, C.; Tan, Y.; Fu, G. C.; Peters, J. C. *J. Am. Chem. Soc.* **2013**, *135*, 9548.
- (32) Fier, P. S.; Hartwig, J. F. *J. Am. Chem. Soc.* **2012**, *134*, 10795.
- (33) (a) Combes, S.; Finet, J.-P. *Tetrahedron* **1999**, *55*, 3377. (b) Tye, J. W.; Weng, Z.; Johns, A. M.; Incarvito, C. D.; Hartwig, J. F. *J. Am. Chem. Soc.* **2008**, *130*, 9971. (c) Tye, J. W.; Weng, Z.; Giri, R.; Hartwig, J. F. *Angew. Chem., Int. Ed.* **2010**, *49*, 2185. (d) Giri, R.; Hartwig, J. F. *J. Am. Chem. Soc.* **2010**, *132*, 15860. (e) Chen, C.; Weng, Z.; Hartwig, J. F. *Organometallics* **2012**, *31*, 8031. (f) Huang, Z.; Hartwig, J. F. *Angew. Chem., Int. Ed.* **2012**, *51*, 1028. (g) Chatterjee, T.; Ranu, B. C. *J. Org. Chem.* **2013**, *78*, 7145. (h) Gurung, S. K.; Thapa, S.; Vangala, A. S.; Giri, R. *Org. Lett.* **2013**, *15*, 5378. (i) Chen, C.; Ouyang, L.; Lin, Q.; Liu, Y.; Hou, C.; Yuan, Y.; Weng, Z. *Chem.—Eur. J.* **2014**, *20*, 657. (j) Chen, C.; Hou, C.; Wang, Y.; Hor, T. S. A.; Weng, Z. *Org. Lett.* **2014**, *16*, 524.
- (34) The final product would then be formed by four reactions occurring at different rates: (i) the original “ligandless” $CuCF_3$ with the free substrate $p-IC_6H_4R$ ($R = CN$ or NO_2), (ii) the original “ligandless” $CuCF_3$ with $[L_m(p-IC_6H_4R)Cu(CF_3)]$, (iii) the free substrate $p-IC_6H_4R$ with $[L_m(p-IC_6H_4R)Cu(CF_3)]$, and (iv) $[L_m(p-IC_6H_4R)Cu(CF_3)]$ as a nucleophile ($Cu-CF_3$) with another molecule of $[L_m(p-IC_6H_4R)Cu(CF_3)]$ as an electrophile (C-I).
- (35) (a) Exner, O.; Böhm, S. *Curr. Org. Chem.* **2006**, *10*, 763. (b) Exner, O.; Böhm, S. *Phys. Chem. Chem. Phys.* **2004**, *6*, 3864. (c) Exner, O.; Böhm, S. *Org. Biomol. Chem.* **2005**, *3*, 1838. (d) Exner, O.; Böhm, S. *Collect. Czech. Chem. Commun.* **2006**, *71*, 1239. (e) Žáček, P.; Dransfeld, A.; Exner, O.; Schraml, J. *Magn. Reson. Chem.* **2006**, *44*, 1073.
- (36) Hansch, H.; Leo, A.; Taft, R. W. *Chem. Rev.* **1991**, *91*, 165.
- (37) Williams, A. L.; Kinney, R. E.; Bridger, R. F. *J. Org. Chem.* **1967**, *32*, 2501.
- (38) Litvak, V. V.; Shein, S. M. *Zh. Org. Khim.* **1974**, *10*, 550.
- (39) Litvak, V. V.; Shein, S. M. *Zh. Org. Khim.* **1974**, *10*, 2360.
- (40) Aronskaya, N. Yu.; Bezuglyi, V. D. *Zh. Org. Khim.* **1974**, *10*, 268.
- (41) Stanko, V. I.; Iroshnikova, N. G. *Zh. Obshch. Khim.* **1979**, *49*, 2076.
- (42) (a) Couture, C.; Paine, A. J. *Can. J. Chem.* **1985**, *63*, 111. (b) Paine, A. J. *J. Am. Chem. Soc.* **1987**, *109*, 1496.
- (43) Strieter, E. R.; Bhayana, B.; Buchwald, S. L. *J. Am. Chem. Soc.* **2009**, *131*, 78.
- (44) Ji, P.; Atherton, J. H.; Page, M. I. *J. Org. Chem.* **2012**, *77*, 7471.
- (45) Foà, M.; Cassar, L. *J. Chem. Soc., Dalton Trans.* **1975**, 2572.
- (46) (a) Ullmann, F. *Ber. Dtsch. Chem. Ges.* **1903**, *36*, 2382. (b) Ullmann, F. *Ber. Dtsch. Chem. Ges.* **1904**, *37*, 853.
- (47) (a) Vorozhtsov, N. N., Jr.; Kobelev, V. A. *Zh. Obshch. Khim.* **1939**, *9*, 1043. (b) Goldberg, A. A. *J. Chem. Soc.* **1952**, 4368. (c) Mayer, W.; Fikentscher, R. *Chem. Ber.* **1958**, *91*, 1536. (d) Vainshtein, F. M.; Tomilenko, E. I.; Shilov, E. A. *Doklady Akad. Nauk SSSR* **1966**, *170*, 1077. (e) Vainshtein, F. M.; Tomilenko, E. I.; Shilov, E. A. *Kinet. Katal.* **1969**, *10*, 777. (f) Lisitsyn, V. N.; Shestakov, V. A.; Sycheva, E. D. *Zh. Vses. Khim. O-va. im. D. I. Mendeleeva* **1969**, *14*, 117. (g) Castro, C. E.; Havlin, R.; Honwad, V. K.; Malte, A.; Moje, S. *J. Am. Chem. Soc.* **1969**, *91*, 6464. (h) Drozd, V. N.; Trifonova, O. I. *Zh. Org. Khim.* **1970**, *6*, 2493. (i) Bruggink, A.; McKillop, A. *Tetrahedron* **1975**, *31*, 2607.
- (48) For reviews, see: (a) Bunnett, J. F.; Zahler, R. E. *Chem. Rev.* **1951**, *49*, 273. (b) Fanta, P. E. *Chem. Rev.* **1964**, *64*, 613. (c) Shein, S. M.; Litvak, V. V. *Zh. Vses. Khim. O-va. im. D. I. Mendeleeva* **1976**, *21*, 274. (d) Lindley, J. *Tetrahedron* **1984**, *40*, 1433.
- (49) (a) Clark, J. H.; McClinton, M. A.; Blade, R. J. *J. Chem. Soc., Chem. Commun.* **1988**, 638. (b) Clark, J. H.; Denness, J. E.; McClinton, M. A.; Wynd, A. J. *J. Fluorine Chem.* **1990**, *50*, 411.
- (50) See, for example: (a) Strieter, E. R.; Blackmond, D. G.; Buchwald, S. L. *J. Am. Chem. Soc.* **2005**, *127*, 4120. (b) Zhang, S.-L.; Liu, L.; Fu, Y.; Guo, Q.-X. *Organometallics* **2007**, *26*, 4546. (c) Kaddouri, H.; Vicente, V.; Quali, A.; Quazzani, F.; Taillefer, M. *Angew. Chem., Int. Ed.* **2009**, *48*, 333. (d) Strieter, E. R.; Bhayana, B.; Buchwald, S. L. *J. Am. Chem. Soc.* **2009**, *131*, 78. (e) Zhang, S.-L.; Ding, Y. *Organometallics* **2011**, *30*, 633. (f) Liu, X.; Zhang, S.-L.; Ding, Y. *Dalton Trans.* **2012**, *41*, 5897. (g) Zhang, S.; Zhu, Z.; Ding, Y. *Dalton Trans.* **2012**, *41*, 13832.
- (51) Extra $Et_3N \cdot 3HF$ is often added to the reagent to enhance its reactivity toward haloarenes.²⁵ HF complexation with $CuCF_3$ can be neglected because of the low computed BDFE of 3.5 kcal/mol.
- (52) Yoke, J. T., III; Weiss, J. F.; Tollin, G. *Inorg. Chem.* **1963**, *2*, 1210.
- (53) We are aware of only one study^{42b} reporting a negative ρ value (-0.25) for Cu-mediated reactions of aryl halides.
- (54) The DFT data-derived correlation coefficient $R^2 = 0.87$ that would be considered unsatisfactory for an experimental Hammett plot is believed to be acceptable for the computational data, especially considering the fact that the barriers calculated for the 11 different $4-RC_6H_4I$ substrates span a very narrow range of 2.5 kcal/mol.
- (55) See, for example: (a) Cioslowski, J.; Liu, G.; Moncrieff, D. J. *Phys. Chem. A* **1997**, *101*, 957. (b) Taskinen, E. *Struct. Chem.* **2000**, *11*, 293. (c) Al-Muhtaseb, A. H.; Altarawneh, M. *Comput. Theor. Chem.* **2011**, *966*, 38. (d) Altarawneh, I.; Altarawneh, M.; Rawadieh, S. *Can. J. Chem.* **2013**, *91*, 999.
- (56) There is no mentioning of two correlations in the previously reported^{16,51} Hammett studies of the reaction of aryl iodides with $CuCF_3$ generated in situ from CF_3CO_2M ($M = Na, K$) with CuI . The limited number of substrates and the high temperatures (160–200 °C) employed in those studies may have made the effect insufficiently noticeable. It is also conceivable that, under such vastly different conditions, the effect is poorly pronounced or absent altogether because of a different nature of the reactive $CuCF_3$ species involved.
- (57) The striking ability of the CF_3 ligand to increase the negative charge or decrease the positive charge on adjacent metal centers has been only recently recognized⁴ and confirmed^{58,59} for a series of various trifluoromethyl transition metal complexes.
- (58) Algarra, A. G.; Grushin, V. V.; Macgregor, S. A. *Organometallics* **2012**, *31*, 1467.
- (59) See also: (a) Goodman, J.; Grushin, V. V.; Larichev, R. B.; Macgregor, S. A.; Marshall, W. J.; Roe, D. C. *J. Am. Chem. Soc.* **2009**, *131*, 4236. (b) Goodman, J.; Grushin, V. V.; Larichev, R. B.; Macgregor, S. A.; Marshall, W. J.; Roe, D. C. *J. Am. Chem. Soc.* **2010**, *132*, 12013.
- (60) (a) Miller, J. *Aromatic Nucleophilic Substitution*; Elsevier: London, 1968. (b) Terrier, F. *Nucleophilic Aromatic Displacement: The Influence of the Nitro Group*; VCH: New York, 1991.
- (61) (a) Miller, J. *Aust. J. Chem.* **1956**, *9*, 61. (b) Miller, J.; Wan, K.-Y. *J. Chem. Soc.* **1963**, 3492.
- (62) (a) Ueda, H.; Sakabe, N.; Tanaka, J.; Furusaki, A. *Nature* **1967**, *215*, 956. (b) Ueda, H.; Sakabe, N.; Tanaka, J.; Furusaki, A. *Bull. Chem. Soc. Jpn.* **1968**, *41*, 2866. (c) Destro, R.; Gramaccioli, C. M.; Simonetta, M. *Acta Crystallogr.* **1968**, *B24*, 1369. (d) Messmer, G. G.; Palenik, G. J. *Acta Crystallogr.* **1971**, *B27*, 314. (e) Gitis, S. S.; Kaminskaya, E. G.; Ivanova, A. I.; Grigor'eva, N. V.; Margolis, N. V.; Kaminskii, A. Ya. *J. Struct. Chem.* **1976**, *17*, 578. (f) Kaminskaya, E. G.; Gitis, S. S.; Ivanova, A. I.; Margolis, N. V.; Kaminskii, A. Ya.; Grigor'eva, N. V. *J. Struct. Chem.* **1977**, *18*, 309. (g) Destro, R.; Pilati, T.; Simonetta, M. *Acta Crystallogr.*

- 1979, B35, 733. (h) Lowe-Ma, C. K. *Acta Crystallogr.* **1986**, C27, 38.
- (i) Niclas, H. J.; Kind, J.; Ramm, M. *J. Prakt. Chem.* **1991**, 333, 909.
- (j) Terrier, F.; Lelievre, J.; Chatrousse, A. P.; Boubaker, T.; Bachet, B.; Cousson, A. *J. Chem. Soc., Perkin Trans. 2* **1992**, 361. (k) Borbulevych, O. Y.; Kovalevsky, A. Y.; Shishkin, O. V.; Atroschenko, Y. M.; Alifanova, E. N.; Gitis, S. S.; Kaminsky, A. Y.; Tarasova, E. Y. *Monatsh. Chem.* **1998**, 129, 467. (l) Alifanova, E. N.; Kaminskii, A. Ya.; Bel'skii, V. K.; Kalnin'sh, K. K.; Tarasova, E. Yu.; Gitis, S. S. *Russ. J. Gen. Chem.* **1998**, 68, 1621. (m) Borbulevych, O. Ya.; Antipin, M. Yu.; Olekhnovich, L. P. *Acta Crystallogr.* **1999**, C55, 2177. (n) Borbulevych, O. Ya.; Shishkin, O. V.; Budarina, Z. N.; Antipin, M. Yu.; Olekhnovich, L. P. *Acta Crystallogr.* **1999**, C55, 1915. (o) Borbulevych, O. Ya.; Shishkin, O. V.; Knyazev, V. N. *Acta Crystallogr.* **1999**, C55, 1704. (p) Borbulevych, O. Ya.; Shishkin, O. V.; Knyazev, V. N. *Acta Crystallogr.* **1999**, C55, 1918. (q) Borbulevych, O. Y.; Antipin, M. Y.; Shishkin, O. V.; Knyazev, V. N. *J. Mol. Struct.* **2000**, 520, 141. (r) Borbulevych, O. Ya.; Antipin, M. Yu.; Shishkin, O. V.; Knyazev, V. N. *Russ. Chem. Bull.* **2000**, 49, 452. (s) Borbulevych, O. Ya.; Shishkin, O. V.; Antipin, M. Yu. *J. Phys. Chem. A* **2002**, 106, 8109. (t) Borbulevych, O. Ya. *J. Chem. Cryst.* **2005**, 35, 777. (u) Galkina, I. V.; Takhautdinova, G. L.; Tudrii, E. V.; Yusupova, L. M.; Krivolapov, D. B.; Litvinov, I. A.; Cherkasov, R. A.; Galkin, V. I. *Russ. J. Org. Chem.* **2013**, 49, 598.
- (63) Thalladi, V. R.; Goud, B. S.; Hoy, V. J.; Allen, F. H.; Howard, J. A. K.; Desiraju, G. R. *Chem. Commun.* **1996**, 401.
- (64) Colapietro, M.; Domenicano, A.; Marciante, C.; Portalone, G. Z. *Naturforsch., B* **1982**, 37, 1309; *Acta Crystallogr., Sect. A* **1981**, 37, C199.
- (65) A considerable contribution of the quinoid form ($C-NO_2 = 1.437(4)$ and $1.429(5)$ Å for two independent molecules) has also been observed for the less accurate structure of *N,N*-diethyl-*p*-nitroaniline: Maurin, J.; Krygowski, T. M. *J. Mol. Struct.* **1988**, 172, 413.
- (66) Talberg, H. J. *Acta Chem. Scand., Ser. A* **1978**, 32, 373.
- (67) (a) Cohen, T.; Wood, J.; Dietz, A. G., Jr. *Tetrahedron Lett.* **1974**, 3555. (b) Cohen, T.; Cristea, I. *J. Org. Chem.* **1975**, 40, 3649. (c) Cohen, T.; Cristea, I. *J. Am. Chem. Soc.* **1976**, 98, 748.
- (68) Ouali, A.; Spindler, J.-F.; Jutand, A.; Taillefer, M. *Adv. Synth. Catal.* **2007**, 349, 1906.
- (69) Zhang, Y.; Ding, Y. *Organometallics* **2011**, 30, 633.
- (70) (a) Casitas, A.; King, A. E.; Parella, T.; Costas, M.; Stahl, S. S.; Ribas, X. *Chem. Sci.* **2010**, 1, 326. (b) Casitas, A.; Canta, M.; Costas, M.; Solà, M.; Ribas, X. *J. Am. Chem. Soc.* **2011**, 133, 19386. (c) Font, M.; Parella, T.; Costas, M.; Ribas, X. *Organometallics* **2012**, 31, 7976.
- (71) For a recent detailed review of Cu(III) complexes in Cu-mediated coupling reactions, see: Casitas, A.; Ribas, X. *Chem. Sci.* **2013**, 4, 2301.
- (72) Dahlén, A.; Petersson, A.; Hilmersson, G. *Org. Biomol. Chem.* **2003**, 1, 2423.
- (73) Frisch, M. J.; Trucks, G. W.; Schlegel, H. B.; Scuseria, G. E.; Robb, M. A.; Cheeseman, J. R.; Scalmani, G.; Barone, V.; Mennucci, B.; Petersson, G. A.; Nakatsuji, H.; Caricato, M.; Li, X.; Hratchian, H. P.; Izmaylov, A. F.; Bloino, J.; Zheng, G.; Sonnenberg, J. L.; Hada, M.; Ehara, M.; Toyota, K.; Fukuda, R.; Hasegawa, J.; Ishida, M.; Nakajima, T.; Honda, Y.; Kitao, O.; Nakai, H.; Vreven, T.; Montgomery, J. A., Jr.; Peralta, J. E.; Ogliaro, F.; Bearpark, M.; Heyd, J. J.; Brothers, E.; Kudin, K. N.; Staroverov, V. N.; Kobayashi, R.; Normand, J.; Raghavachari, K.; Rendell, A.; Burant, J. C.; Iyengar, S. S.; Tomasi, J.; Cossi, M.; Rega, N.; Millam, N. J.; Klene, M.; Knox, J. E.; Cross, J. B.; Bakken, V.; Adamo, C.; Jaramillo, J.; Gomperts, R.; Stratmann, R. E.; Yazyev, O.; Austin, A. J.; Cammi, R.; Pomelli, C.; Ochterski, J. W.; Martin, R. L.; Morokuma, K.; Zakrzewski, V. G.; Voth, G. A.; Salvador, P.; Dannenberg, J. J.; Dapprich, S.; Daniels, A. D.; Farkas, Ö.; Foresman, J. B.; Ortiz, J. V.; Cioslowski, J.; Fox, D. J. *Gaussian 09, Revision D.01*; Gaussian, Inc., Wallingford CT, 2009.
- (74) (a) Grimme, S. *J. Comput. Chem.* **2004**, 25, 1463. (b) Grimme, S. *J. Comput. Chem.* **2006**, 27, 1787.
- (75) Cancès, M. T.; Mennucci, B. B.; Tomasi, J. *J. Chem. Phys.* **1997**, 107, 3032.
- (76) Andrae, D.; Haussermann, U.; Dolg, M.; Stoll, H.; Preuss, H. *Theor. Chim. Acta* **1990**, 77, 123.
- (77) Höllwarth, A.; Böhme, M.; Dapprich, S.; Ehlers, A. W.; Gobbi, A.; Jonas, V.; Köhler, K. F.; Stegmann, R.; Veldkamp, A.; Frenking, G. *Chem. Phys. Lett.* **1993**, 208, 237.
- (78) Hariharan, P. C.; Pople, J. A. *Theor. Chim. Acta* **1973**, 28, 213.
- (79) Fukui, K. *Acc. Chem. Res.* **1981**, 14, 363.
- (80) Schwabe, T.; Grimme, S. *Phys. Chem. Chem. Phys.* **2006**, 8, 4398.
- (81) Ehlers, A. W.; Böhme, M.; Dapprich, S.; Gobbi, A.; Höllwarth, A.; Jonas, V.; Köhler, K. F.; Stegmann, R.; Veldkamp, A.; Frenking, G. *Chem. Phys. Lett.* **1993**, 208, 111.
- (82) Frisch, M. J.; Pople, J. A.; Binkley, J. S. *J. Chem. Phys.* **1984**, 80, 3265.
- (83) Rappé, A. K.; Casewit, C. J.; Colwell, K. S.; Goddard, W. A.; Skiff, W. M. *J. Am. Chem. Soc.* **1992**, 114, 10024.